Electrophysiology of inhibition and auditory prediction mechanisms in human cortex

By

Yvonne M. Fonken

A dissertation submitted in partial satisfaction of the

requirements for the degree of

Doctor of Philosophy

in

Neuroscience

in the

Graduate Division

of the

University of California, Berkeley

Committee in charge:

Professor Robert T. Knight, Chair
Professor Frederic E. Theunissen
Professor Richard B. Ivry
Professor Bin Yu

Fall 2017

Abstract

Electrophysiology of inhibition and auditory prediction mechanisms in human cortex

By

Yvonne M. Fonken

Doctor of Philosophy in Neuroscience

University of California, Berkeley

Professor Robert T. Knight, Chair

One of the core problems the brain has to solve is how to navigate and interact with the external world. This requires a complex analysis of sensory input, the translation of perceptual input to goal-directed behavior, followed by motor planning and execution. In this thesis we investigated two crucial aspects of this perception-action cycle. First, we examined the underlying neural mechanisms that support response inhibition. Here, novel sensory information is integrated on very short time-scales to cancel an already planned action. The frontal cortex is believed to play a crucial role in the temporal organization of goal-directed behavior and cognitive control and is implicated in stopping a motor response. Using the high spatiotemporal resolution of electrocorticography (ECoG), we found evidence for two distinct processes localized to the middle frontal gyrus (MFG). High-frequency band (HFB) power increased in stop-trials before the stop-signal reaction time (SSRT), showing no difference between successful and unsuccessful stops. We interpret this activation as contributing to the stopping process, either by signaling the stop-signal itself, or by implementing attentional control. A second HFB activation was observed after the go and stop processes have finished, and was larger for unsuccessful stops, and is likely related to behavioral monitoring. Our results support the notion that frontal cortex implements different functions related to stopping.

Implementing the perception-action cycle not only involves re-acting to novel information from the senses in a bottom-up manner. It is believed that the brain also implements a strategy anticipating future events based on prior knowledge. Here we investigated how anticipation of sounds influences auditory processing. Using both EEG and ECoG, we employed a task with omissions of expected sounds, thereby isolating endogenous responses to expectations in

auditory cortex. We found that a subset of auditory active electrodes in lateral superior temporal gyrus (STG) and superior temporal sulcus (STS) showing HFB power increases to omissions. We were able to successfully decode whether the subject heard the syllable 'Ba' or 'Ga'. However, which sound was omitted could not be decoded from auditory active sites, nor from the omission HFB increase specifically. We also observed a negative ERP in posterior STG in the intracranial data, which may be related to an auditory cortical generator of the N2 component. In a separate EEG studies we also observed both an N2 negativity, as well as a negativity occurring before the intracranial negativity, the source of which may be in A1, a region which we could not access intracranially. Finally, a P3a ERP was observed in EEG, which points to both the HFB and ERP effects in posterior STG to be signatures of auditory-specific salience or mismatch detection.

Dedicated to

My parents, Els & Jan
-
For their endless support

My partner Matthew
-
For keeping me grounded

Table of Contents

Acknowledgments

Although this work has my name on it, there have been a great number of people that have contributed, and without whom this work would not have been possible. To start, I would like to thank all patients who have selflessly and generously contributed their time to this research. Their motivation to participate is an inspiration, and I would like to express my deepest appreciation.

I would also like to thank my advisor Bob Knight, for being my mentor for the last seven years. With your help I matured to a well-rounded researcher, and I appreciate the independence you have giving me during my PhD to pursue my interests in auditory prediction. Not only did you teach me about science and the brain, you also made sure I would leave Berkeley with more knowledge and enthusiasm for American sports, and especially the outdoors. Thank you for everything that you have done for me.

I also thank all Knight lab members and collaborators from 2009-2017, as well as the HWNI administrators. I have learned a lot from all of you, and received support in one form or another from each of you. I would like to specifically thank Ulrike, Matar, and Julia for your mentorship at different times during my PhD. I also thank Francine for allowing time to talk about research and less serious matters. I also thank my thesis committee, consisting of Frederic Theunissen, Richard Ivry and Bin Yu, for their input and guidance. I would also like to acknowledge my funding sources, including Fulbright for granting me a scholarship for 2012-2013, the Helen Wills Neuroscience Institute, HHMI for granting me their predoctoral international student fellowship for 2014-2017, and the NIH for funding my research through R01 funds granted to the Knight lab. I also thank the UC field station reserve system and its managers, including the Angelo Coast reserve, the Quail Ridge reserve and the Yosemite field station, for providing me with the best writing retreat locations possible.

This thesis would not have happened without the help of a great number of people. For Chapter 2, I would like to acknowledge the instrumental role Ulrike Kramer played in all stages of the study. In addition, I thank Jochem, Elinor, Kira and Nicole for their contributions, as well as Nathan Crone, Josef Parvizi, and Eddie Chang for their help with accessing and recording from patients. For Chapter 3 and 4 I would like to acknowledge Chris Holdgraf for helping me get set-up with doing my analyses in python. I also thank Jack Lin, Peter Brunner, Gerwin Schalk and his team for their help with accessing and recording from patients. I thank Peter for his help getting my task running in Albany, and for being available to answer my data-

related questions. For Chapter 3 I thank Arjun and Christine for their rotation work on exploring the data. For Chapter 4 I would like to acknowledge Eena, Inga Marie, and Rebecca for work on the EEG study. Finally, I would like to acknowledge Michelle, Howard and Janna, for their work not directly related to this thesis. I also thank Richard, Sandon, Cal, Kira, and Jamie for their help with electrode reconstructions and other support.

My biggest supporters throughout my PhD were my parents, who have taught me the importance of education and scholarship, and have been incredibly supportive of my somewhat unconventional plan to move to the other side of the world to learn more about the brain. I would also like to thank my extended family and friends for their continuous support. Of my friends, I would like to name two special individuals, Bregje and Katelyn. Thank you Bregje for allowing our friendship to grow despite the large distance. Katelyn, thank you for being my friend, and sharing the ups and downs of graduate school with me. Both of you have been there for me throughout my PhD, and I could not have done it without your support. I also thank James and Sam for being there for me, especially during the last, and hardest, few months of writing my dissertation.

To conclude, I would like to thank the most important person in my life, my partner Matthew. You have been there for me, and supported me through the hardest parts of my PhD, for which I can never thank you enough. You know me better than anyone, you have helped me grow, and you have kept me grounded when I needed it the most. I love you, and I am looking forward to continue to grow with you.

Chapter 1: Introduction

'*Here we have the most miraculous mass of protoplasm on this earth, and perhaps in our galaxy. Its potential is virtually unknown'*.
– Dr. Marian Diamond (1926-2017) on the human brain.

The complexity of the brain and its function is indeed astounding, and we may never understand it completely. With this work I hope to contribute to furthering our knowledge of the human brain, knowing that I stand on the shoulders of giants like Dr. Diamond.

Any approach of trying to understand the brain will not do justice to its complexity, though some approaches can be useful. The focus of this thesis is the cerebral cortex. The cerebral cortex is part of the brain that is largely responsible for what makes humans special in terms of our cognitive functional capabilities. The cortex is characterized as large sheets of neurons organized in layers, and is sub-divided in primary sensory cortices, higher order sensory cortices, association cortex and motor cortex (Gazzaniga et al., 2002). In primary sensory regions information from the senses enters the cortex after passing through a number of sub-cortical structures. Sensory cortex is mostly hierarchically organized, each level representing increasingly complex features. In association cortex, information from different senses is integrated with internal goals, and interfaces with the motor cortex to generate behavior to interact with the environment. This describes what is called the perception-action cycle, a view that a central function of the brain is to continuously navigate the interaction between perception and action (Fuster, 2013). However, localizing specific functions to specific brain structures, like the practice of phrenology from 150 years ago (Zola-Morgan, 1995), would be overly simplistic. Rather, current thought views the brain as operating with widely distributed and interconnected networks. Indeed, within the hierarchical structures in cortex there are a multitude of recurrent connections, as well as interactions that are not strictly hierarchical (Fuster, 2013). Specific regions of the brain can still be characterized as functional 'units', but also need to be understood in terms of their place in a larger network and its interactions with other regions (Fuster, 2013).

In this thesis, we focus on illuminating specific aspects of the perception-action cycle. **Chapter 2** examines frontal contributions to motor inhibition using the stop-signal task, a unique showcase in which the perception-action cycle at work. Here, a motor action in the form of a button press is prepared in response to a 'go' signal.

Sometimes this go-signal changes color, indicating that the subject needs to inhibit their movement. This requires a fast integration of novel sensory information with the current task-set, and the implementation of the cancelation of an action. In addition to rapidly responding to novel information, an important aspect of the perception-action cycle lies in anticipating events based on experience (Fuster, 2013). **Chapters 3 and 4** therefore focus more specifically on predictive processes in perception as evidenced by their influence on auditory processing. To isolate expectation-related physiological activations from sensory-evoked signals, we studied omissions of expected sounds.

Inhibitory motor control and the role of lateral frontal cortex

The ability to rapidly update motor output in response to novel information is included in the greater definition of cognitive control, a function ascribed to frontal cortex (Neubert et al., 2013). Response inhibition has been interpreted conceptually with the help of the horse race model, in which the largely independent go and stop processes 'race' each other, and the process finishing first determines the outcome (Boucher et al., 2007; Logan et al., 1984). The cortical network associated with response inhibition includes right inferior frontal gyrus (rIFG), primary motor cortex (M1), and the pre-supplementary motor area (pre-SMA) (Aron et al., 2007b; Neubert et al., 2013). The stopping process initiated in cortex then interacts with subcortical motor structures included in the basal ganglia, specifically through the subthalamic nucleus (STN) (Aron et al., 2007b). The involvement of rIFG in stopping has been established with studies using fMRI (Garavan et al., 1999), TMS (as reviewed by Neubert et al. 2013), ECoG (Bartoli et al., 2017; Swann et al., 2009, 2012a, 2012b), and human lesion studies (Aron et al., 2004; Krämer et al., 2013).

The precise role of the IFG is not well understood, and it has been suggested that it is involved with response inhibition directly, or contributes indirectly through attentional control (Neubert et al., 2013). Some argue that the IFG is involved in response inhibition as part of the ventral attention network (Duann et al., 2009). This right-lateralized network encompasses regions such as the temporoparietal junction (TPJ), insula, left cingulate and SMA (Corbetta and Shulman, 2002; Downar et al., 2000), and its main function is believed to signal behaviorally relevant stimuli, and draw attentional resources to salient events. This network interacts with the dorsal attention network, which is primarily involved with goal-directed (or top-down) attention (Corbetta and Shulman, 2002). The question arises as to whether IFG involvement in inhibitory motor control is due to the salient, infrequent nature of the stop signal (Neubert et al., 2013). One interpretation is that the role of the rIFG is to implement an attentional capture, serving a stop-detection function, and subsequently alerts pre-SMA to signal the inhibition of a planned movement to STN (Duann et al., 2009; Sharp et al., 2010).

The rIFG could also have subregions implementing different functions, explaining both seemingly contrasting interpretations of its function in response inhibition. It has been shown that different parts of IFG are active in response to inhibition, as well as salience and feedback processing (Chikazoe et al., 2009). Finally, other regions in lateral frontal cortex have been shown involvement in response inhibition. Primary motor cortex shows an interruption of motor preparation for successful stops (Swann et al., 2009), inhibition-related activations in middle frontal gyrus (Garavan et al., 1999), as well as in DLPFC (Chikazoe et al. 2009; Swann, Tandon, et al. 2012).

Chapter 2 will focus on lateral frontal cortex, and investigate specific contributions from IFG and other frontal regions including M1, DLPFC and middle frontal gyrus (MFG). The initial approach was to compare successful to unsuccessful stops, which proved useful in finding some contributions to inhibition in M1 and DLPFC. However, the surprising finding in the experiment described in **Chapter 2** is that the MFG, not the IFG becomes active in stop trials regardless of the outcome, providing additional insight in contributions of other regions in lateral frontal cortex.

Prediction and the Brain

The idea of the brain as a prediction machine, first proposed by Helmholtz (Olshausen, 2014), has become increasingly popular over the last two decades. This view describes how perception and action are aided by predictions and expectations generated by the brain based on prior knowledge. It is seen as a unifying model of the brain, in which higher order regions in the cortex interact with lower-order regions hierarchically through a multitude of recurrent connections communicating predictions (Clark, 2013). Currently there are two main approaches to the brain implementing a predictive scheme describing top-down feedback signals. One is a hierarchical Bayesian inference framework as described by Lee & Mumford (2003), which interprets feedback to facilitate lower-level processing consistent with the prediction, whereas inconsistent signals are suppressed. In contrast, predictive coding describes predictions playing a role to cancel out activity at lower levels, as described by Rao and Ballard (1999) with respect to the visual system. In this view feed-forward signals carry the residual error between the prediction and the actual input, also called prediction error (PE) (Rao and Ballard, 1999). This has since then been integrated into the free-energy principle based model by Karl Friston (Friston, 2010). This model follows the predictive coding idea by Rao and Ballard (1999), casts it as an energy conservation approach of the brain through minimizing surprise (Friston, 2010).

Examples of such prediction-related suppression of brain responses have been shown in fMRI (Kok et al. 2012; Alink et al. 2010; Murray et al. 2002; but see St.

John-saaltink et al. 2015), and MEG/EEG (Summerfield et al., 2011; Todorovic et al., 2011). Evidence of prediction-error signals are characterized as larger sensory cortical responses to surprising stimuli, as well as responses to omissions of expected stimuli (Arnal and Giraud, 2012). However, these methods are based on the summation of activity of large numbers of neurons, and facilitation effects may average out. Indeed, fMRI studies have shown that despite a reduction in the BOLD response expected gratings are more easily decoded from V1 (Kok et al., 2012), and expected gratings that were omitted can be retrieved from V1 BOLD activations (Kok et al., 2014). The question remains whether the brain uses predictions to implement a cancellation or a facilitation process

Chapters 3 and **4** examine the mechanism of prediction by examining the role of predictive information on auditory processing. To isolate predictive processes from sensory evoked responses, we specifically examine omissions of expected sounds. Questions asked in **Chapter 3** are whether we can localize omission activations to auditory regions, if this behaves as a prediction-error according to predictive coding models, and if this activation resembles a template of the expected stimulus. I will show omission high-frequency band (HFB) activations recorded with ECoG in auditory regions, which provide important insights both to the prediction literature as well as the organization of the auditory cortex along the anterior-posterior axis. **Chapter 4** focuses on event-related potentials (ERP) to omissions from EEG studies, relating it with a long history of omission and saliency-related recorded potentials.

Organization of human auditory cortex

From the hair cells in the ear, auditory signals travel through a number of subcortical structures before it reaches auditory cortex in the temporal lobe, with delays as short as 30ms (Liegeois-Chauvel et al., 1994). Auditory cortex consists of primary auditory cortex (A1), located on Heschl's gyrus, and secondary regions in the belt and parabelt areas surrounding A1, extending into the lateral surface of the superior temporal gyrus (STG) (Schnupp et al., 2011). A1 is organized as a tonotopical map, reflecting the organization of the basilar membrane in the ear (Humphries et al., 2010). The dorsal superior temporal gyrus (STG) is believed to be involved with acoustic analyses, and respond more strongly to complex sounds compared to noise (Binder et al., 2000; Gazzaniga et al., 2002; Hickok and Poeppel, 2007). The superior temporal sulcus has been implicated with phonological processing, and responds more to speech sounds compared to non-speech sounds (Hickok and Poeppel, 2007). Regions responsible for word comprehension include the middle temporal gyrus, temporal pole, inferior temporal gyrus and angular gyrus (Binder et al., 2000, Canolty et al, 2007). In addition to defining a hierarchy of sound processing, it has been suggested that the auditory cortex is organized in a

dorsal- and ventral stream. Some interpret anterior regions of the STG as being involved with auditory object processing, and posterior regions with analyzing space and motion (Bizley and Cohen, 2013). Others have characterized these two streams as a dorsal stream mapping acoustic speech signals to frontal networks, whereas the ventral stream processes speech signals for comprehension (Hickok and Poeppel, 2007). The results shown in **Chapter 3** provide new evidence for a differential specialization of auditory cortex along the anterior-posterior axis.

Electrophysiology of human cortex

The study of the electric fields produced by the human brain started almost a hundred years ago, when Hans Berger recorded the first electroencephalogram (EEG) in 1929 (Berger, 1929). The EEG is a recording of the brain electric potential arising from populations of neurons, and is measured by placing electrodes on the scalp. Excitatory and inhibitory postsynaptic potentials create extracellular current sinks and sources. If this occurs coherently, these field potential fluctuations can be measured on the scalp (Nunez and Srinivasan, 2006). Electric field potentials can also be measured intracranially. This typically happens in surgical patients, most commonly in patients with epilepsy undergoing pre-surgical monitoring. Jasper and Penfield were some of the first to do intracranial studies (Jasper and Penfield, 1949). In EEG, the skull acts both as a low-pass temporal and spatial filter. The skull is a poor conductor of electricity, which causes spatial smearing of the electric fields. Signals with higher temporal frequencies are believed to also occur at higher spatial frequencies, which cancel out more easily with combined spatial smearing and decreased amplitude from volume conduction. As a result, the EEG only reliably records temporal frequencies up to ~50Hz (Nunez and Srinivasan, 2006). The advantage of intracranial recordings is that signals can be measured at higher spatio-temporal resolutions compared to EEG. Indeed, intracranial recordings show physiological signals at frequencies between 50-200Hz in addition to <50Hz frequencies observed in EEG (Crone et al., 1998a, 1998b). The loss of high frequency activity at the scalp if quantified by the well know 1/f function.

A significant contribution of physiological signals to the EEG are oscillatory in nature, and different frequencies have been grouped functionally into frequency bands. The frequency bands that will be discussed here are beta (13-30Hz), and high-gamma, or high-frequency band (HFB; 70-150Hz). Beta oscillations are observed most prominently over motor cortex, and have been related to motor preparation and inhibition processes (Engel and Fries, 2010; Pfurtscheller and Lopes da Silva, 1999). The oscillatory nature of the high-gamma band, or high-frequency band (HFB), is debated (Hermes et al., 2015; Miller et al., 2007). Neuronal oscillations are characterized by a narrow-band peak in the power spectrum,

whereas HFB activity appear as a broad-band phenomenon (Miller et al., 2007), which has been related to neuronal firing (Manning et al., 2009; Ray and Maunsell, 2011, Rich and Wallis, 2017). Increases of HFB power are therefore considered to reflect local cortical activations, and are distinct from lower frequency gamma oscillations in the 30-60 Hz range (Ray and Maunsell, 2011), and may receive contributions primarily from local and long-range incoming action potentials (Miller et al., 2009). HFB signal also correlates with the BOLD signal in fMRI (Logothetis et al., 2001), though under specific conditions (Hermes et al., 2017). In addition to frequency-band focused analyses, EEG research historically has focused on event-related potentials (ERP's), i.e. deflections of the electric field potential related to an event. Some of these ERP's can only be extracted by averaging many trials. Although ERP's have been a useful tool in Cognitive Neuroscience experiments, their origins and mechanisms are still relatively unknown (Nunez and Srinivasan, 2006). To address this gap in the literature In **Chapter 4** I include a comparison of ERP's observed in healthy subjects using EEG, and intracranial ERP's recorded in patients.

Chapter 2: Frontal and motor cortex contributions to response inhibition: evidence from electrocorticography

*This chapter is based on the following publication:
Fonken et al, '*Frontal and motor cortex contributions to response inhibition: evidence from electrocorticography'*, Journal of Neurophysiology 115: 2224-2236 (2016)

Abstract

Changes in the environment require rapid modification or inhibition of ongoing behavior. We used the Stop-Signal paradigm and intracranial recordings to investigate response preparation, inhibition and monitoring of task relevant information. Electrocorticographic data (ECoG) was recorded in eight patients with electrodes covering frontal, temporal and parietal cortex, and time-frequency analysis was used to examine power differences in the beta (13-30 Hz) and high-gamma bands (60-180 Hz). Over motor cortex, beta power decreased and high-gamma power increased during motor preparation for both Go trials and unsuccessful stops. For successful stops, beta increased and high-gamma was reduced, indexing the cancellation of the prepared response. In the middle frontal gyrus (MFG), stop-signals elicited a transient high-gamma increase. The MFG response occurred before the estimated stop signal reaction time, but did not distinguish between successful and unsuccessful stop-trials, likely signaling attention to the salient stop-stimulus. A post-response high-gamma increase in MFG was stronger for unsuccessful compared to successful stops and absent in go-trials, supporting a role in behavior monitoring. These results provide evidence for differential contributions of frontal sub-regions to response inhibition including motor preparation and inhibitory control in motor cortex, and cognitive control and action evaluation in lateral prefrontal cortex.

Introduction

Response inhibition is an essential cognitive control function needed to withhold unwanted motor behavior. Deficits in response inhibition are observed in many neuropsychiatric disorders including attention-deficit/hyperactivity disorder or obsessive-compulsive disorder, as well as in patients with damage to prefrontal cortex (Aron et al., 2004; Chamberlain et al., 2006; Krämer et al., 2013; Lijffijt et al., 2005). Functional imaging, electrophysiological data and lesion studies implicate a network of prefrontal, parietal and subcortical regions in response inhibition (Aron, 2011; Aron and Verbruggen, 2008; Boucher et al., 2007). However, the precise role and temporal dynamics of activity in these different regions is uncertain (Munakata et al., 2011).

Attempts to elucidate the specific role of different brain regions can be guided by a separation of the agent, i.e. the source of inhibitory activity or where the inhibitory process is instigated, the site at which inhibitory activity is exerted and the manifestation, i.e. where and how the result of the inhibitory activity can be measured (Band and Boxtel, 1999). While the agent of inhibition is usually assumed to be within the prefrontal cortex or basal ganglia, the site of inhibition might be within thalamus or M1 and be manifested in a a change of activity in inhibited trials compared to uninhibited trials (Band and Boxtel, 1999; Mattia et al., 2012). One influential model proposes a three-pronged network comprising right inferior frontal gyrus (rIFG), subthalamic nucleus (STN) and the pre-supplementary motor area (pre-SMA) as critical agents for stopping (Aron et al., 2014, 2007a). Others have stressed the role of the pre-SMA and STN together with the striatum rather than the rIFG in stopping (Munakata et al., 2011; Schmidt et al., 2013). The picture might be even more complex as some recent studies have shown that both STN need to be activated to stop an action (van den Wildenberg et al., 2006; Mirabella et al., 2012). Finally, transcranial magnetic stimulation (TMS) studies have demonstrated inhibitory activity within M1, suggesting $GABA_B$ mediated intra-cortical inhibition as a possible manifestation of stopping (Coxon et al., 2006; van den Wildenberg et al., 2010). This observation fits with event-related potential- (ERP) findings from ECoG recordings in patients performing a stop-signal task revealing stopping-specific ERP components in M1 and premotor cortex (Mattia et al., 2012). Neurophysiological recordings in monkeys during manual go-no go or stop-signal tasks have also reported stopping-related activity in several areas implicated in response selection during goal-directed action, including the pre-SMA (Matsuzaka and Tanji, 1996; Shima et al., 1996; but see Scangos and Stuphorn, 2010), the STN (Isoda and Hikosaka, 2008) and dorsal premotor cortex (Kalaska and Crammond, 1995; Mattia et al., 2013; Mirabella et al., 2011). This suggests that there is considerable overlap between the networks involved in action preparation and action inhibition

(Mirabella, 2014). However, comparisons between species must be made with caution as connectivity and functional specialization of prefrontal areas might differ.

Here, we used the unique spatio-temporal resolution of intracranial electrophysiological (electrocorticography, ECoG) recordings in humans to investigate the dynamics of cortical neural activity during inhibitory motor control. Recordings were obtained from patients with refractory epilepsy who had electrode grids or strips implanted for 4 – 10 days to localize seizure foci and perform cortical stimulation mapping. Electrodes were located over prefrontal, motor, temporal or parietal areas of either the right or left hemisphere. Patients performed a visual stop-signal paradigm (SSP) (Logan et al., 1984), which is a well-established paradigm used to study response inhibition. In the SSP, participants perform a choice reaction time task in which a stop-signal is infrequently presented after the go-signal, indicating the need to stop the already prepared response. The latency of the stopping process, referred to as the stop-signal reaction time (SSRT), is estimated based on the reaction-time distribution and the likelihood of inhibition (Logan, et al., 1984).

Previous ECoG studies employing the stop-signal task focused on the rIFG (Swann et al., 2009) and on activity and connectivity between pre-SMA and rIFG (Swann et al., 2012a). Swann et al. (2009) reported a beta power increase at rIFG electrodes in inhibited stop-trials relative to failed inhibitions. In a second ECoG study (Swann et al., 2012a), a beta power increase in stop-trials was observed over pre-SMA and rIFG electrodes. Together with EEG and behavioral data from Parkinson's disease patients on and off DBS STN stimulation (Mirabella et al., 2012; Ray et al., 2009; Swann et al., 2011; van den Wildenberg et al., 2006), these researchers hypothesized an inhibitory network involving rIFG, STN and pre-SMA, which is indexed by beta oscillations. This hypothesis has been questioned by others (Schall and Godlove, 2012), because the rIFG beta response seemed to vary between patients. Previous ECoG studies on a cued stop-signal task have also focused on power changes in high-gamma, which included stop-related activations in pre-SMA (Swann et al., 2012a) and task-set related activations in ventrolateral PFC and dorsolateral PFC after both the cue and the go-signal (Swann et al., 2012b).

In the present study we present a more extensive dataset (8 patients) with coverage of both left and right PFC. We assessed both changes in activity in the beta band, as well as power changes in the high gamma range (60 – 180 Hz). High gamma power changes have been shown to mark local cortical activity in various sensory, motor and cognitive tasks (Crone, Miglioretti, Gordon and Lesser, 1998; Edwards et al., 2005; Flinker et al., 2011) and to correlate with neuronal spiking activity (Cardin et al., 2009; Ray and Maunsell, 2011). High-gamma activations in PFC have been reported before in a cued stop-signal task (Swann et al., 2012b) in relation to the cue and go stimuli. In the current paper, we analyzed prefrontal high-gamma activity to

the stop-stimulus to assess more specifically the role of PFC regions in reactive motor inhibition.

We hypothesized that brain regions involved in inhibitory motor control, i.e. agent and site of inhibition, should show differential high gamma activity for successful and unsuccessful stop-trials in the time-range before the estimated SSRT (Schall and Godlove, 2012). To address this, we first examined responses in the primary motor cortex (M1) as the putative cortical site of inhibition, where we hypothesized a high-gamma power increase (Crone et al., 1998a) and a beta decrease (Swann et al., 2009; Zhang et al., 2008) related to the motor response. For successful stops, we predicted a reduced response in the high-gamma band, as local cortical activity in M1 should be suppressed as a result of the stopping process. We then examined high gamma activity over prefrontal cortex to assess the temporal dynamics of MFG and IFG activity related to motor preparation, inhibition and monitoring. We also examined beta changes over prefrontal sites, to test the hypothesis that a beta-dependent fronto-basal ganglia network is involved in stopping (Swann et al., 2009, 2012a).

Methods

Participants

Eight patients (Fig 2.1a; Table 2.1, appendix A; seven men; mean age 27.5 years) undergoing neurosurgical treatment for medically refractory epilepsy participated in the study. Patients were implanted with one or more electrode arrays, with electrode placement and other medical decisions solely determined by the clinical needs of the patient. The patients were monitored for 4-7 days post-implantation. During lulls in clinical evaluation, the patients performed the SSP task while electrophysiological signals were recorded. Written and oral informed consent was obtained according to the Declaration of Helsinki. Three subjects (S01-03) were recruited from the University of California, San Francisco (UCSF) Hospital. Subjects had their epilepsy medications reduced or discontinued while being monitored. Four subjects (S04-07) participated at Johns Hopkins Hospital and one subject (S08) participated at Stanford Hospital. The study was approved by the UCSF, Stanford, UC Berkeley and Johns Hopkins committees for human research. All subjects had normal or corrected-to-normal vision. All but one (S08) had some prefrontal coverage (four right, four left, Figure 2.1A). Note that S04 had bilateral prefrontal coverage (left hemisphere not shown on Figure). The location of the electrode grids and strips were reconstructed by realigning a pre-operative anatomical MRI scan and a post-implant CT scan using BioImage Suite® software. Note that the precision of this method may vary by up to one centimeter due to small changes in the shape of the brain after grid electrode implantation.

Paradigm and experimental procedures

The stop-signal task was a manual choice reaction time task (Logan, et al., 1984), wherein a visual stop-signal is presented on 25% of the trials (Fig. 2.1B). The go-signal was a white arrow pointing either to the right or to the left, requiring a corresponding mouse button press from the signaled hand. Patients performed the task with the hand contralateral to the electrode grid or strips (this was the dominant hand in 3 cases). In stop-trials, the go-signal was followed by a stop-signal (arrow color changed to red) after a delay. Subjects were instructed to press the corresponding button when a go-signal appeared, and to inhibit this response when the stop-signal was presented. They were instructed to react as fast and as accurately as possible. Stimulus duration was 400ms and inter-trial duration was jittered between 1.0 and 1.2s. The stop-signal delay was initially set to 150ms, and adjusted online using a staircase-tracking algorithm to ensure a stopping probability of about 50% (Levitt, 1971, Aron et al., 2007). To achieve this, if the patient made an error, the stop-signal delay increased by 16 ms and it decreased by 16 ms after successful inhibitions. Stop-signal delays could range between 20ms and 380ms.

The task was programmed in Presentation® and was presented on a laptop. The task was practiced first to ensure that patients fully understood and followed the task instructions.

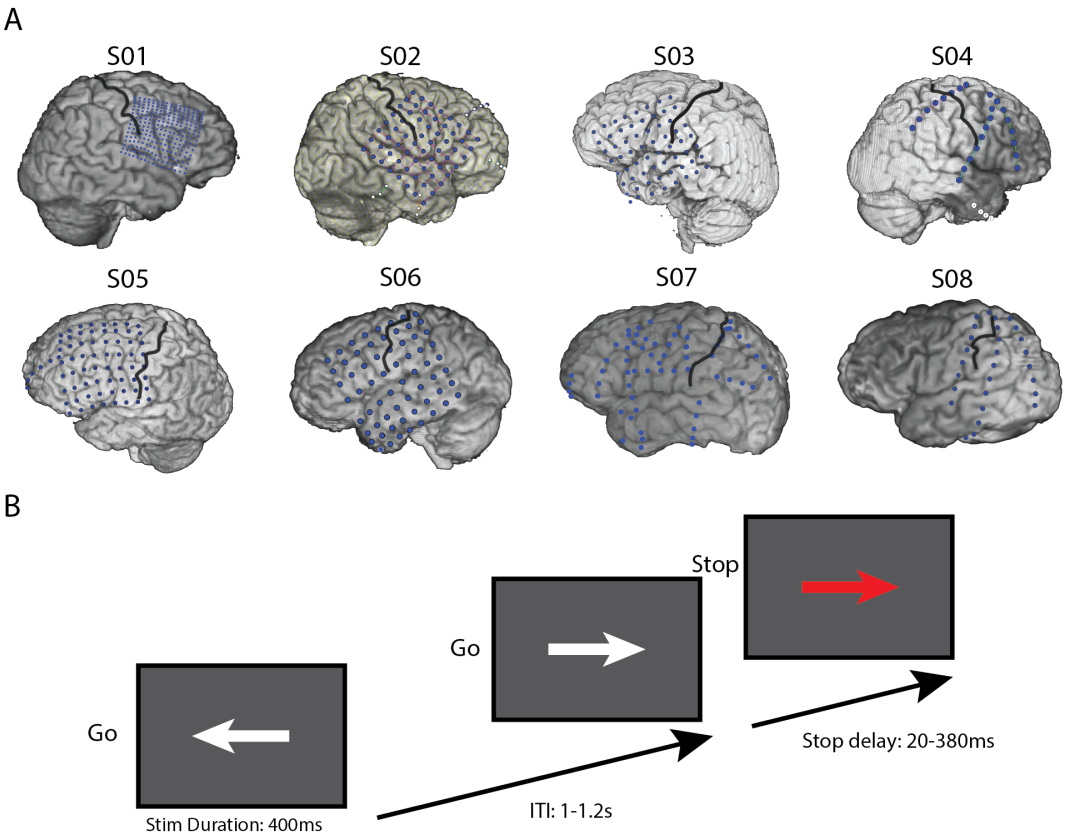

Figure 2.1 A) CT and structural MRI reconstructions of individual subject electrode coverage. Black line denotes the central sulcus. Note that S04 had bilateral prefrontal strips (left side not shown). Note also that the grid for S03 has shifted ~1cm anterior after the CT was done, based on motor and auditory responses from a different task run in this subject (data not shown). The original CT-MR reconstruction shown here does not reflect this suspected shift B) Schematic of the stop-signal task used in the present study; ITI inter trial interval

ECoG recording

The data was recorded at three different sites using either a Tucker Davis Technologies recording system (patients recorded at Stanford and UCSF) or Stellate Harmony amplifier (Stellate Systems, Inc., Montreal, Canada; Johns Hopkins patients). The electrophysiological channels were sampled at 3.051 kHz (Stanford, UCSF) or 1 kHz (Johns Hopkins). A subdural electrode was used as reference electrode and a scalp electrode was used as ground during data acquisition. The electrode grids (Pt-Ir electrodes with 2mm exposed diameter) had 1 cm inter-electrode spacing, except the high-density grid of one patient with a 16x16 grid with

4 mm spacing (S01). The electrode grids were manufactured by Ad-Tech Medical Instrument Corporation.

Data analysis

Preprocessing

For offline signal-processing we used functions from the EEGlab toolbox (Delorme and Makeig, 2004) and the chronux toolbox (http://chronux.org) (Mitra and Bokil, 2007) in combination with custom-written Matlab® code. The data was down-sampled to 1kHz after standard anti-alias filtering. Electrodes were excluded from the data if they showed 60 Hz line noise, epileptic activity or other artifacts such as excessive noise due to poor contact. Electrodes were also excluded if their variability exceeded the average variability across electrodes by more than two standard deviations. All epochs with spread of epileptic activity from the primary epileptic site were also excluded from analysis. No corrections were made for eye-movements or muscular artefacts, as no EOG or EMG channels could be recorded. Although eye-movement artifacts may contaminate frontal ECoG electrodes, they mostly affect frequencies lower than the range we focused on (13-200Hz) (Ball et al., 2009). The data was subsequently de-trended with a high-pass filter of 0.5Hz and segmented into three conditions: correct go-trials (Go), successful stops (SS) and unsuccessful stops (US). Finally, the data was re-referenced using a common average reference method (CAR).

Time-Frequency Analysis

Single-trial signal changes in the time-frequency domain were computed by estimating the analytic amplitude around a specific frequency through convolution with a complex Morlet wavelet with a spectral bandwidth of centerfrequency/2π, using 41 center-frequencies logarithmically spaced between 2 and 200 Hz. We focused on the high-gamma band (60 – 180 Hz) and the beta band (13 – 30Hz). For the spectrograms, the percent signal change in the beta or high-gamma range was computed relative to the pre-stimulus baseline (-200 to -50ms). Differences between conditions were assessed after averaging the data in 10ms time-windows for a time-window of 0-800ms after the relevant stimulus and above-mentioned frequency bands. Statistical testing was done on raw (i.e. non-baselined) single trial power traces based on a within-subject design, and the number of trials were matched by randomly taking subsets trials of the condition with the most trials. Note that the figures show the data in power percent change versus baseline for visualization purposes only. Statistical significance was determined with a nonparametric statistical test (Wilcoxon signed rank test) and corrected for multiple comparisons using a false discovery rate (FDR) of $p < 0.05$. All reported results were FDR corrected (Benjamini and Hochberg, 1995) unless stated otherwise. As FDR

correction is relatively conservative, we also reported uncorrected results as to prevent false negatives. Uncorrected results were deemed significant and mentioned if three consecutive 10ms time-bins had a p-value smaller than 0.01. Electrode selection was done by pre-defined anatomical regions, namely primary motor cortex, IFG, and MFG. When multiple electrodes showed a similar effect, we chose to present the time-courses of one representative electrode in the figures.

Results

Behavior

Reaction times in go-trials ranged from 430ms to 660ms (526ms ± 34ms, mean and SEM). The reaction time for unsuccessful stop-trials (US; 445ms ± 25ms; $t_6 = 5.26$, $p<0.01$, paired t-test) was shorter compared to Go trials for each subject, which is to be expected since it is more likely to make an error when responding faster. The staircase algorithm adapted the stop signal delay to on average 185ms ± 26ms for successful stop-trials (SS) and 204ms ± 25ms for US. The average probability of failure was 49.4% (41 – 53%). The latency of stopping (or stop signal reaction time; SSRT) was 302ms ± 31ms, which is still within the range observed in the stop signal task in previous ECoG studies (Swann et al., 2009, 2012a). We also calculated reaction time changes after stop- compared to go-trials as the difference in response time after go- or stop-trials relative to the preceding trial (Krämer et al., 2011). All subjects showed post-error slowing, i.e. how much the subject slows down in go trials after compared to before stop trials (average difference in RT is 59ms ± 10 SEM; $t_6 = 5.8$, $p<0.01$, paired t-test), and were faster after SS trials (average difference in RT is -64ms ± 21 SEM; $t_6 = -3.1$, $p<0.05$, paired t-test). Note that faster RTs after successful inhibitions are in line with previous findings from our lab (Krämer et al., 2011), but are not consistently found. In fact, whether a post-inhibition-slowing or -speeding is found seems to depend on the way the post-stop-slowing is calculated, i.e. as difference relative to average go-trials or difference relative to stop-preceding go-trial (see Krämer et al., 2011 for further discussion). Individual behavioral results are reported in Table 2.2 (appendix A).

Motor related changes in the beta and high-gamma bands in M1

We first investigated motor related beta and high-gamma changes in the primary motor cortex. Four patients had coverage of the M1 hand area (one over right hemisphere) and the results for an M1 electrode and the topography of power changes across all electrodes from a patient with a high-density grid (4 mm spacing) are shown in Figure 2.2. Data for the other subjects with 1 cm electrode separation are shown in Figure 2.3. In trials with a motor response (Go and US), we observed a high-gamma (60-180 Hz) power increase and a beta (13-30 Hz) desynchronization in the time-window of 200 ms before the motor response until 200 ms after the motor response (relative to a 200 ms baseline before the go-stimulus). As can be observed in Figure 2.2B, the beta decrease was more widespread across the sensorimotor cortex whereas the high-gamma increase was focused at only very few electrodes. We first discuss effects for both frequency bands relative to pre-stimulus baseline (-200ms to -50ms before the go or stop stimulus) and then present the results of condition differences. The reported effects were significant after FDR

correction at p < 0.05 unless stated otherwise (see also Methods). Note that the topographic maps in Figure 2.2B (and following figures) show power changes for all electrodes independently of statistical significance. For Go trials, effects were significant for all 4 subjects and for 3 of 4 subjects they were significant in US events (p<0.01, uncorrected, for US high-gamma in S06). For SS trials, the high-gamma response was reduced or absent. Beta power increased in SS trials relative to baseline (S01 p<0.01, uncorrected; S08 p<0.05, FDR corrected) did not change from baseline (S06), or a decreased relative to baseline was observed instead (S03 p<0.05, FDR corrected; Fig. 2.3).

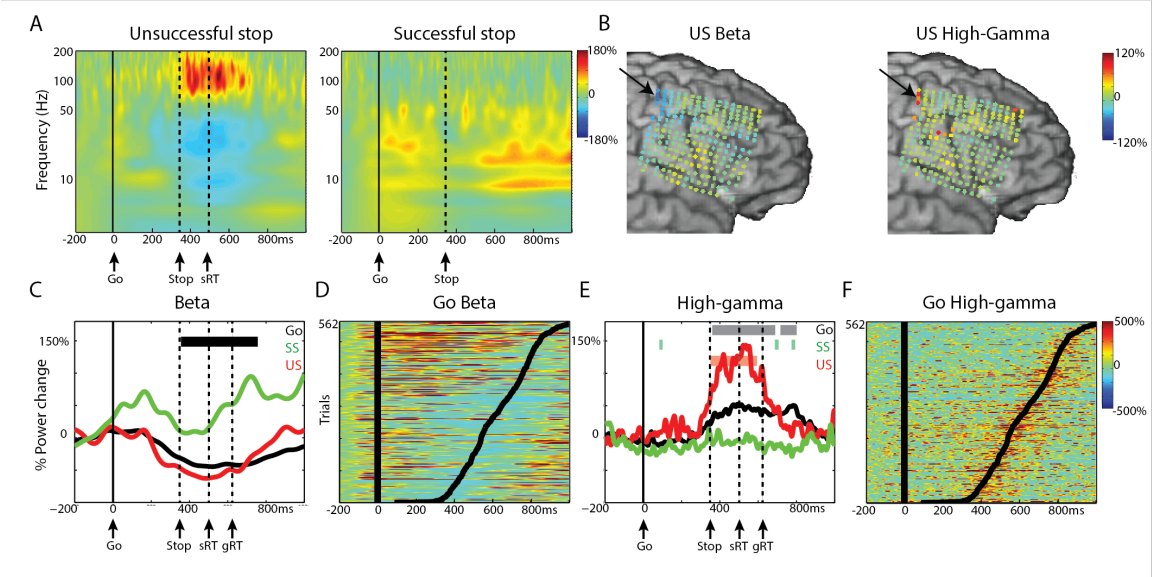

Figure 2.2 High-gamma and beta effects in M1 for patient S01. A) Time-frequency average for the three conditions, time-locked to the go-signal. Dashed vertical lines show the mean reaction time for go (gRT) or US (sRT) and the mean stop signal delay (Stop). B) Beta (left) and High-Gamma power changes for US shown for all electrodes. Data shown is time-locked to the response and averaged over -50ms to 50ms relative to the response time. Arrow indicates the location of electrode shown in other panels in this figure C) Time-course for mean beta power in the three conditions, go (black), successful stop (SS, green) and unsuccessful stop (US, red). The horizontal black bar indicates the time-window with a significant difference between US and SS (p<0.05, FDR corrected) D) Beta power for single trials for the go-condition, sorted by reaction time (black line) E) Time-course plot for high-gamma power in the three conditions. Colored bars indicate the time-windows with significant differences compared to baseline (p<0.05, FDR corrected) F) High-gamma power for single trials for the go-condition, sorted by reaction time (black line).

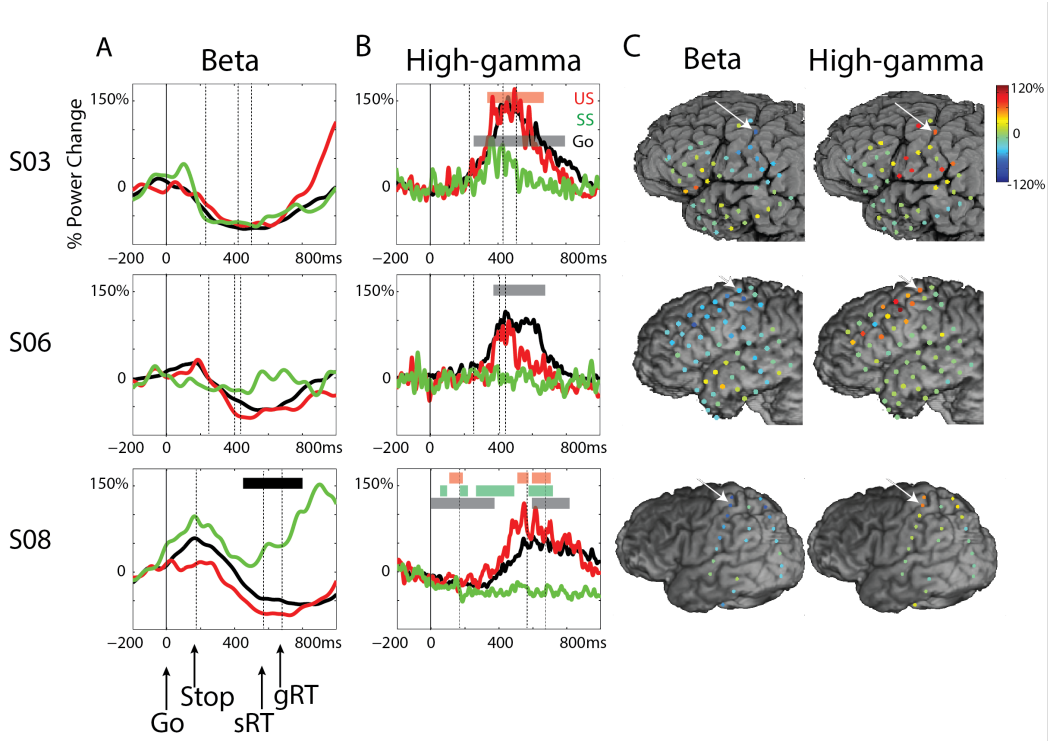

Figure 2.3 Beta and high-gamma time-courses for M1 for subjects S03, S06 and S08. A) Time-course plots for beta power in the three conditions go (black), successful stop (SS, green) and unsuccessful stop (US, red). Horizontal black bar signifies the time-window with a significant difference between US and SS ($p<0.05$, FDR corrected) B) Time-course plots for high-gamma power in the three conditions. Dashed vertical lines indicate the average time-point of the stop-signal, the reaction time in unsuccessful stop-trials (sRT) and reaction time in go-trials (gRT). Colored bars signify the time-window with significant differences compared to baseline ($p<0.05$, FDR corrected). C) Beta (left) and High-Gamma power changes for US shown for all electrodes. Data shown is time-locked to the response and averaged over -50ms to 50ms relative to the response time. The arrow indicates the location of electrodes shown in other panels in this figure**.**

Next, we look at significant differences between conditions. For S01 and S08 we observed an early increase of beta power around 100ms and a beta rebound around 700ms after the go-signal, the latter was significantly different between SS and US (Fig. 2.2C; 2.3A), as well as between SS and Go trials. Notably, the power in the alpha-band (8-13Hz) (Pfurtscheller and Neuper, 1994) shows a similar time-course as the beta-band (Figure 2.2A), as well as a similar topography as the beta-band (beta topography shown in Figure 2.8). High-gamma increases in Go and US were significant compared to SS in all subjects ($p<0.01$, uncorrected for S03 and S06). Single trial power traces for go-trials sorted by reaction time (Fig. 2.2D and F) show that the effects in both frequency bands are consistent over trials and centered around the reaction time (sRT). The high gamma response was transient and started 125ms ±83ms (latency of significant high-gamma power vs baseline, N=4) before the response. Note that these motor preparation and execution high-gamma effects

are not necessarily limited to one electrode, especially as seen in the high-density grid (Figure 2.2B). The effects reported here confirm previous findings of beta desynchronization and high-gamma power increases in M1 during motor preparation and execution (Babiloni et al., 2016; Crone et al., 1998a, 1998b; Pfurtscheller and Lopes da Silva, 1999; Swann et al., 2009). Notably, the effects were quite consistent for high gamma whereas the beta effects were more heterogeneous which has been reported previously (Crone et al., 1998a, 1998b).

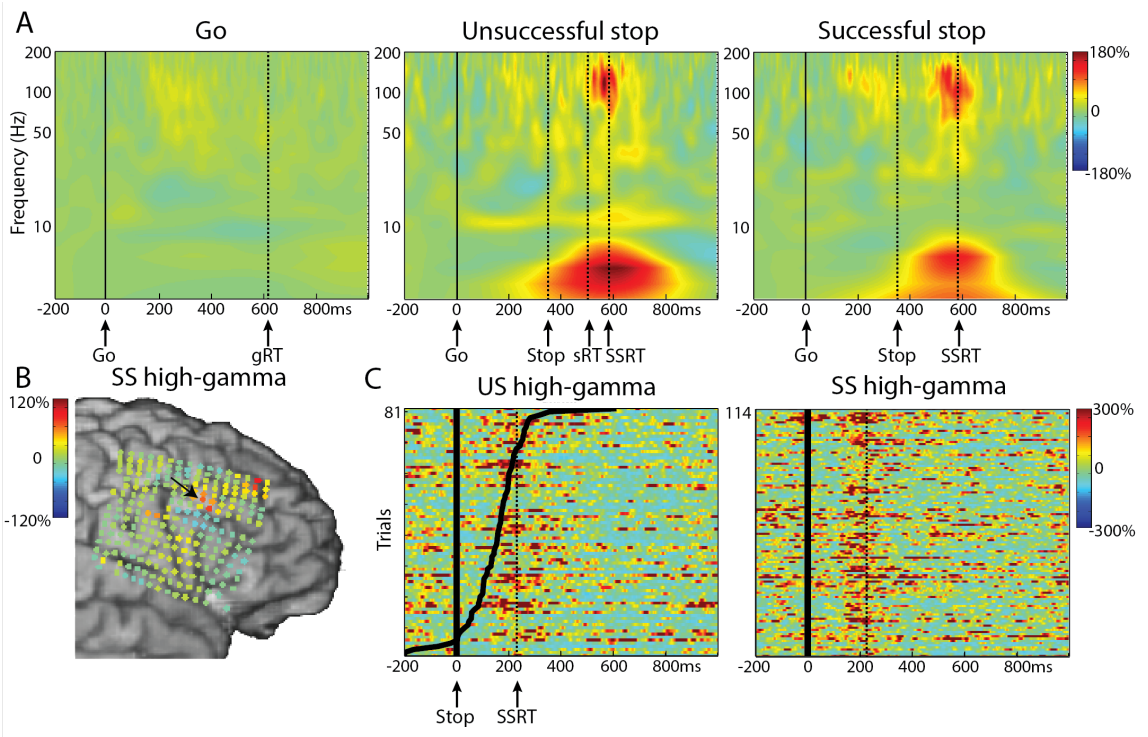

Figure 2.4 Stop-related high-gamma effects in the middle frontal gyrus for S01. A) Time-Frequency plots for the three conditions, time-locked to the go-signal. Dashed vertical lines reflect the mean reaction time for go (gRT) or US (sRT), the mean stop signal delay (stop) and the stop signal reaction time (SSRT). B) High-gamma power changes for SS shown for all electrodes. Data shown is time-locked to the stop-signal and averaged over -50ms to 50ms relative to the SSRT. Arrow indicates the location of electrode shown in other panels in this figure C) High-gamma power for single trials for both stop conditions, time-locked to the stop signal, sorted by reaction time (black line). The dotted vertical line is the SSRT.

Early stop-related high-gamma responses in MFG

In stop trials, we observed a high-gamma increase over both right and left MFG that was significant versus baseline. This effect was found in all five subjects with substantial frontal coverage ($p<0.01$ uncorrected for SS in S03). As an example, time-frequency plots in Figure 2.4A show this transient high-gamma increase for both SS and US conditions for the subject with the high density 4 mm grid (S01). This was consistent over trials and occurred after the stop-stimulus as can be assessed from the stop-signal locked data (Fig. 2.4C). Note that the high gamma

response was accompanied by an increase in the theta band. Figure 2.4B shows the high-gamma power change in the time-window of -50ms to 50ms around the estimated SSRT in stop-signal locked data, for successful stop-trials across all electrodes. The high-gamma increase is localized to a few electrodes close to the inferior frontal sulcus. Note also the high-gamma increase in the anterior-superior corner of the grid, which is further described later in this paper (Fig. 2.6).

In Figure 2.5, the mean high-gamma time-course is shown for all five subjects. The stop-related high-gamma response was observed in electrodes located in the middle frontal gyrus varying in exact location across subjects (Fig. 2.5C). The high-gamma response was absent in go-trials (S01, S02, S03) or diminished (S05, S06). The high-gamma response for stop-trials was larger compared to Go trials for all subjects (Fig. 2.5A; $p<0.05$; FDR corrected, this was only significant at an uncorrected level of $p < 0.01$ in S03 SS), but high-gamma amplitude did not differ between SS and US-trials. Note also that the stop-signal-related high-gamma power increase started about 120ms before the end of the estimated SSRT (HG was significant vs baseline, $p <0.05$, FDR corrected, at 111ms ± 58ms before SSRT for US; 136ms ± 62ms for SS; $t_3 = 3.9$, $p = 0.03$) and was maximal prior to the end of the SSRT (Fig. 2.5A and B). For one patient (S03) this effect was observed in a more posterior site compared to other patients. We may be missing activation site that occurs more anterior, where we do not have coverage. For S03, a high-gamma increase was also observed at more inferior frontal and parietal sites (Figure 2.5C), but this was not seen in the other two patients with coverage of these areas (S05, S06).

Stop-signals in the SSP are less frequent than go-signals and neural responses to the stop-signal might be modulated by this difference in stimulus probability. To investigate whether the early MFG response reflected the tracking and updating of local stimulus probabilities, we performed a post-hoc analysis of the relationship between the high-gamma amplitude in these electrodes with the number of go-trials preceding the stop trial. This analysis revealed no significant correlations ($t_{499} = 0.28$, $p=0.63$, linear mixed effects model, with HG amplitude as the dependent variable, number of go-trials preceding the stop trial as the independent variable, and subject as random effect).

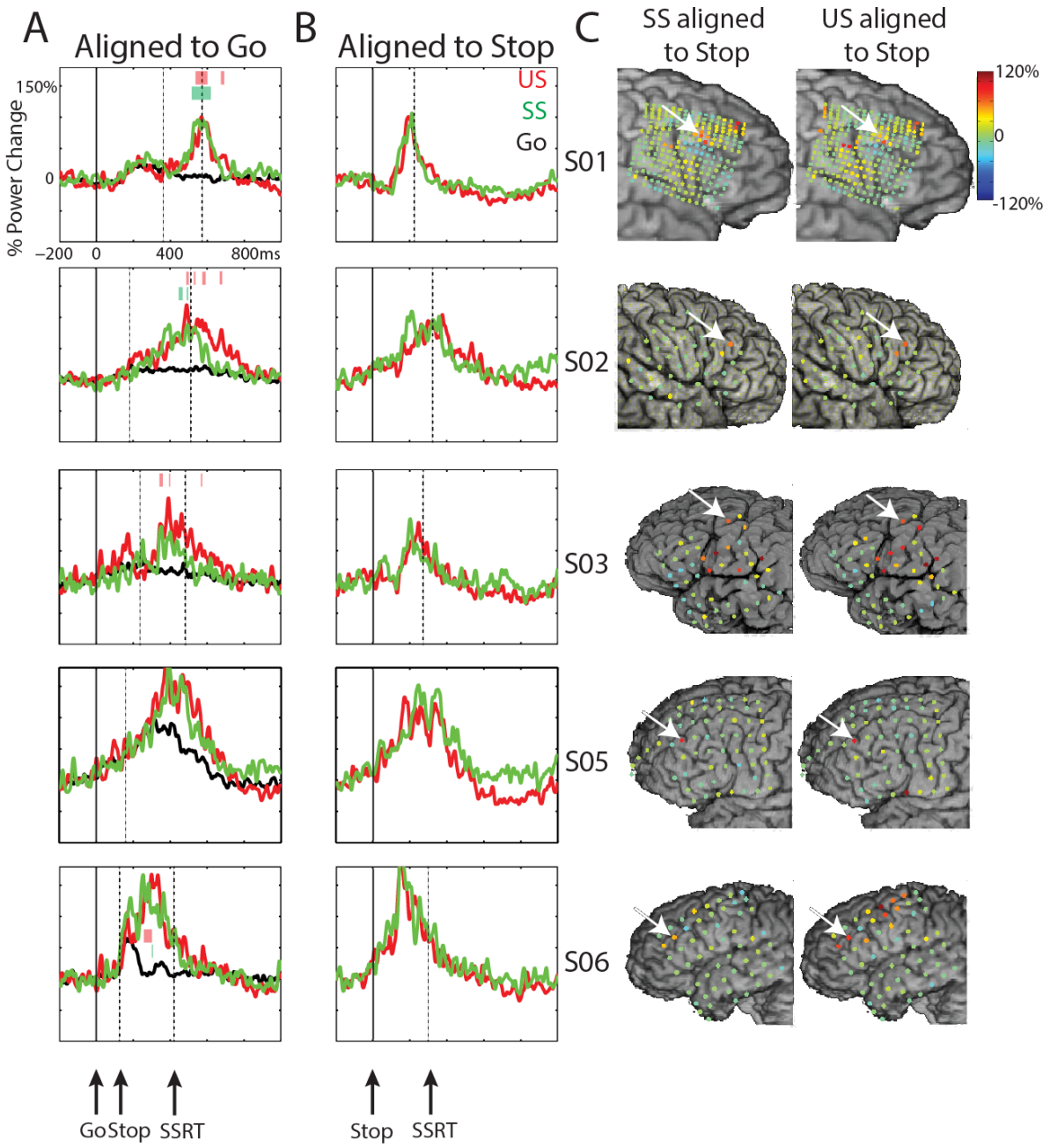

Figure 2.5 Stop-related high-gamma effects in the middle frontal gyrus for S01, S02, S03, S05 and S06. A) Time-courses for high-gamma power aligned to the go-signal for the three conditions: go (black), successful stops (SS; green) and unsuccessful stops (US; red). Dashed vertical lines reflect the mean stop signal delay (Stop) and the stop signal reaction time (SSRT). Colored bars signify time-windows for differences between SS and Go (green) and US and Go (red) ($p<0.05$, FDR corrected) B) Time-courses for high-gamma power aligned to the stop-signal for SS and US C) High-gamma power changes for SS and US shown for all electrodes. Data shown is time-locked to the stop-signal and averaged over -50ms to 50ms relative to the SSRT. For S05 the data was taken from 150 to 250ms after the stop signal for visualization purposes only, as the actual SSRT is not known. Arrow indicates the location of electrode shown in other panels in this figure

Post-response, stop-related high-gamma in middle frontal gyrus

A longer latency high-gamma increase for stop trials was recorded in the MFG in two subjects (S01 and S07). Figure 2.6A shows that the high-gamma increase was absent in go-trials, but increased versus baseline for both stop conditions for S01, and for US in S07. The high-gamma signal was also increased for US versus SS and US vs Go ($p<0.01$, uncorrected for S07). This high gamma response occurred after the motor response in US trials (Fig. 2.6B). The electrode showing the effect in S01 was located more anterior in the MFG (and close to the superior frontal sulcus) compared to the electrode site for S07. Figure 2.6C shows the topography of high-gamma power changes in the time-window of 0ms to 200ms after the response, demonstrating the very focal high-gamma response at few electrodes in S01 and one electrode in S07. This late MFG response was strongest after failed inhibitions, suggesting a behavioral monitoring effect. Such monitoring of performance in the MFG in stop-trials might be related to behavioral adaptation after stop-trials, particularly after unsuccessful inhibitions. We examined a possible relation between the MFG high-gamma response and the amount of post-error slowing across trials. This post-hoc analysis showed no significant differences ($t_{56} = -0.21$, $p=0.83$, linear mixed effects model, with HG amplitude as the dependent variable, the amount of post-error slowing as the independent variable, and with subject as a random effect, 2 subjects). Note also that the high gamma response was almost absent in successful stop-trials (Figure 2.6). In fact, in S07 only a late high gamma *decrease* relative to baseline yielded significance. Interestingly, patients showed a decrease of reaction times after successful stop-trials in contrast to an RT increase after stop-errors (see Table 2.2, appendix A).

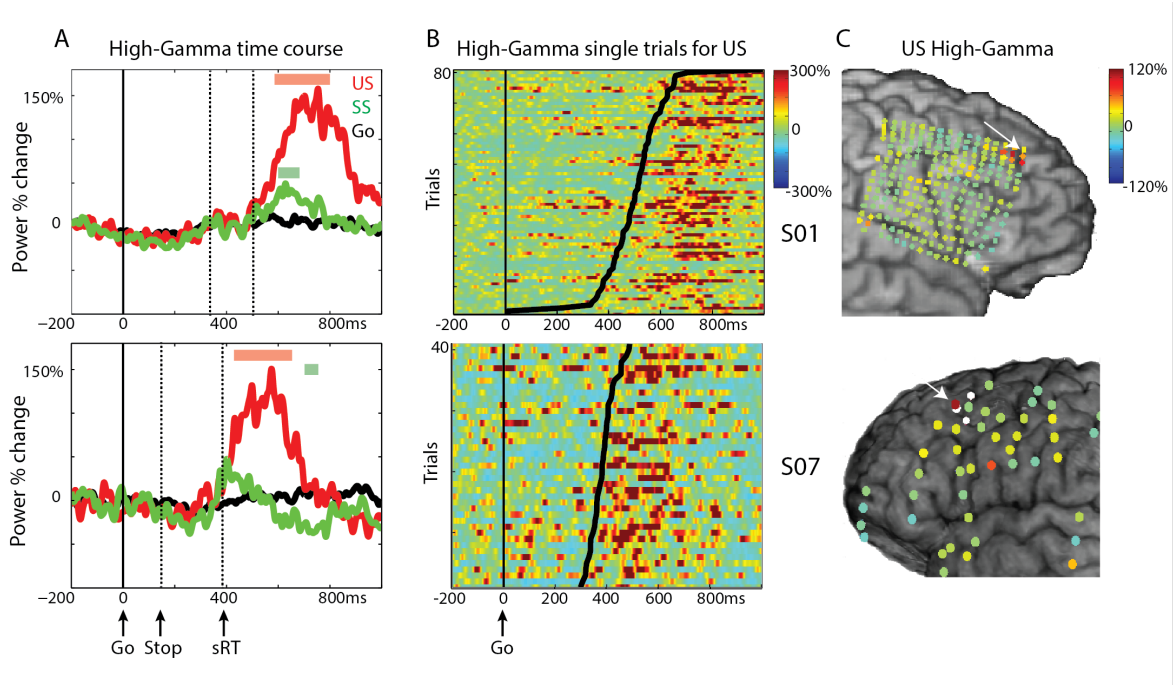

Figure 2.6 Late high-gamma response in MFG for S01 and S07. A) Time-courses for high-gamma power aligned to the go-signal for three conditions: go (black), successful stops (SS; green) and unsuccessful stops (US; red). Dashed vertical lines reflect the mean stop-signal delay (Stop) and the reaction time for US (sRT). Colored bars indicate significant high-gamma increases compared to baseline for US (red) and SS (green) ($p<0.05$, FDR corrected). B) High-gamma power for single trials for US, aligned to the go-signal, sorted by reaction time (black line). C) High-gamma power changes for US shown for all electrodes. Data shown is time-locked to the response time and averaged over 0ms to 200ms relative to the motor response. Arrow indicates the location of electrode shown in other panels in this figure

Stop-related changes in the beta-band

In addition to the beta-changes in M1, we observed beta band effects for three subjects in sites around the central and precentral sulci (S01) and parietal cortex (S08; Fig. 2.7A) and in the IFG/MFG in both left and right hemispheres (S01, S05; Fig. 2.7B). Generally, stopping-related beta effects in the prefrontal cortex were more heterogeneous across subjects than the high gamma response. In the central sulcus/parietal sites, beta increased during SS. For S01, beta power increased after the SSRT, whereas in S08 beta power was increased throughout the trial. In both subjects this increase was stronger in SS compared to US and go conditions. Note that the electrode in S01 is several electrode rows anterior and inferior to the M1 site reported in this paper.

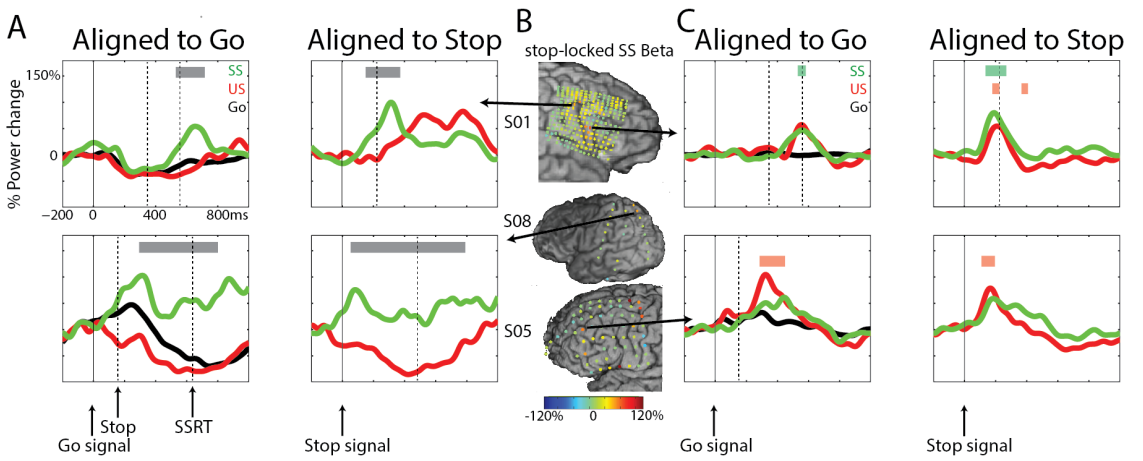

Figure 2.7 Changes in beta power for subjects S01, S05 and S08. A) Time-courses for beta power aligned to go and stop signals for peri-central sulcus sites for three conditions: go (black), successful stops (SS; green) and unsuccessful stops (US; red). Dashed vertical lines reflect the stop-signal and the stop signal reaction time (SSRT). Grey bars signify time-windows for differences between SS and US ($p<0.05$, FDR corrected) B) beta power changes for SS shown for all electrodes. Data shown is time-locked to the stop-signal and averaged over -50ms to 50ms relative to the SSRT. Arrow indicates the location of electrode shown in other panels in this figure C) Time-course for beta power aligned to go and stop signals for IFG/MFG sites for three conditions. Colored bars indicate time-windows for differences between SS (green), US (red) vs. baseline ($p<0.05$, FDR corrected)

The beta increase over IFG/MFG sites was apparent in both stop conditions and no significant differences between SS and US were found. Figure 2.7B shows the beta power changes for all electrodes in S01, S05 and S08. The beta effects for both subjects were significant versus baseline for SS ($p<0.01$ uncorrected for S05), and for US ($p<0.05$, FDR corrected for S01 stop-locked only; S05 both go and stop-locked). A third subject with extensive right IFG coverage (S02) showed no significant beta changes in any of the IFG electrodes (data not shown). Note in Figure 2.7C that the beta response for subject S05 was found in the same electrode as the stop-related high gamma response described earlier (Fig. 2.5). Finally, to provide an overview of the complete stop-related time-course of beta and high gamma changes, Figure 2.8 shows the averaged relative power changes for patient S01 separately for successful und unsuccessful stop-trials. The effects described above are highlighted with arrows.

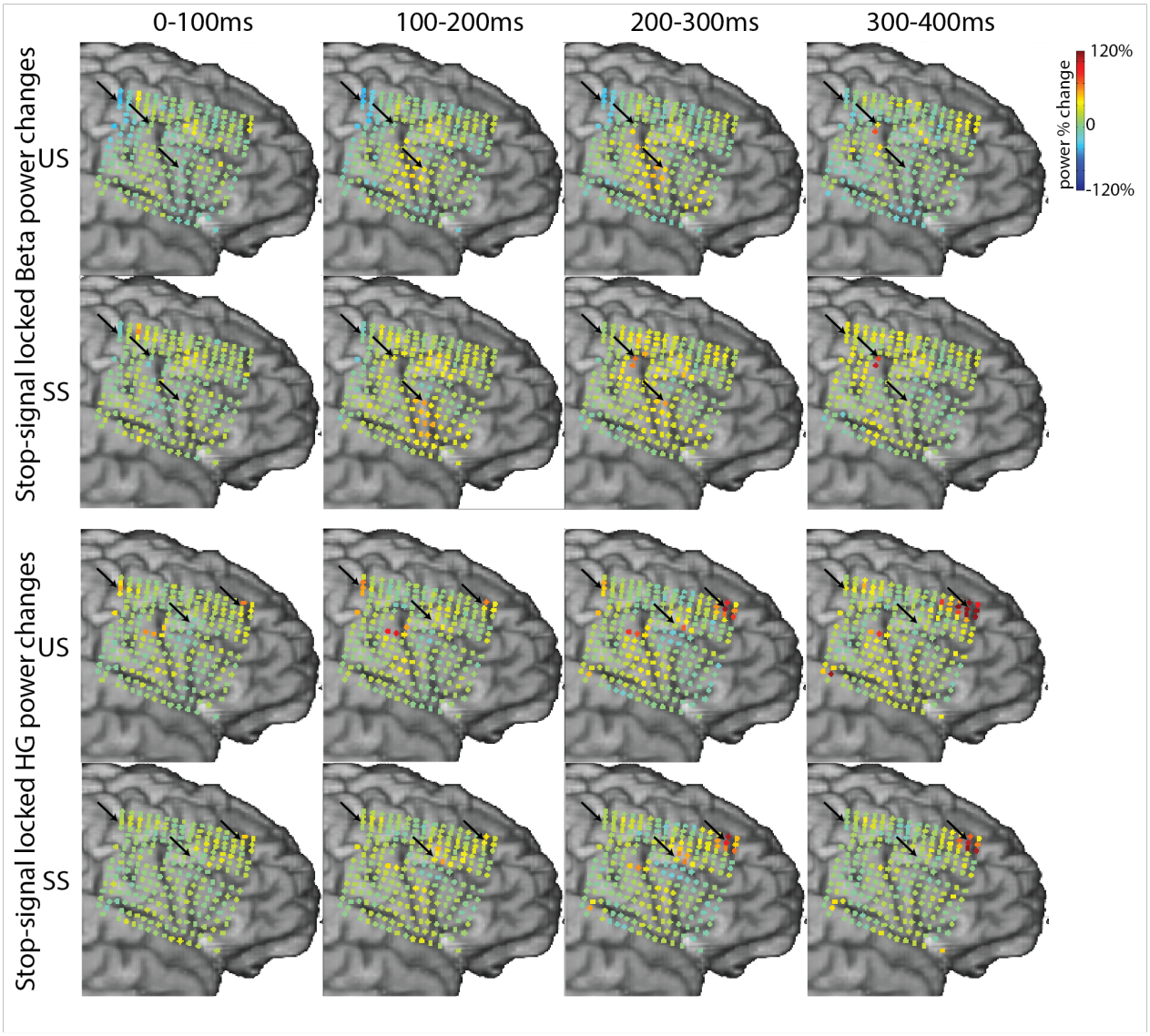

Figure 2.8 Beta and High-Gamma power changes overview for subject S01. The data is time-locked to the stop signal (0ms) and averaged over 100ms for four consecutive time-windows. The marked electrodes correspond to the electrodes presented in Fig. 2.2, 2.7 for the Beta panels, and Fig. 2.2, 2.4, 2.5, 2.6 for the HG panels.

Discussion

We examined oscillatory dynamics over lateral frontal cortex related to inhibitory motor control in a stop-signal task in patients with subdural grid electrodes. We observed two distinct effects in lateral PFC during stop-trials. A transient high-gamma increase, maximal before the SSRT, was found in MFG. This response did not differ between SS and US and may reflect an attention process triggered by the salient, behaviorally relevant stop-signals. A later high-gamma increase in more rostral MFG was evident after motor responses and was larger for US compared to SS, suggestive of action monitoring of incorrect behavior. We confirmed previous findings in the primary motor cortex, showing a beta decrease and high-gamma increase related to motor preparation and execution, and a beta rebound and absence of high-gamma changes for successfully inhibited responses. In contrast to previous findings, analyses of stop- related beta changes in IFG or MFG could not reveal significant differences between SS and US (Swann et al., 2009).

Motor preparation activity and inhibitory effects in M1

Motor preparation in M1 sites was associated with a beta-band decrease and a high-gamma increase (Fig. 2.2 + 2.3) relative to a pre-stimulus baseline and maximal around the time of movement execution. This is in line with findings from non-invasive studies (as reviewed by Pfurtscheller and Lopes da Silva, 1999) as well as ECoG studies (Crone et al., 1998a, 1998b; Miller et al., 2007). For SS our data confirmed a beta rebound, i.e. a power increase after an initial decrease, similar to that shown before in human ECoG (Swann et al., 2009) and animal studies (Zhang et al., 2008). Expanding on this, we observed a smaller or absent high-gamma response in SS. Note that the beta rebound in SS was found in two patients only and was not observed for patient S03, who also showed a small, yet statistically not significant increase in high-gamma in this condition. This patient may not have fully inhibited the motor response, but inhibited it sufficiently enough to prevent a button press. However, since we did not record EMG this remains speculative.

The observed differences between successful and unsuccessful stops indicate that M1 is either downstream of the site of inhibition, which may be located in subcortical sites (Mirabella et al., 2012; van den Wildenberg et al., 2006; Zandbelt and Vink, 2010) or premotor cortex (Mattia et al., 2013, 2012; Mirabella et al., 2011), or is the site of inhibition itself (Band and Boxtel, 1999). This would be in line with recent empirical and theoretical work attributing the causal role in motor inhibition to the (pre)-motor cortex and suggesting that response preparation and inhibition are subserved by specific interactions in strongly overlapping networks (Mirabella, 2014; Mirabella et al., 2011; Mattia e al., 2013).

Attentional control and monitoring of behavior in the MFG

The first prefrontal effect we observed was a transient stop-related high-gamma power increase (Fig. 2.4+2.5) in both the right and left MFG. This increase was seen for stop-trials compared to go-trials in all subjects with extensive coverage of the prefrontal cortex (N=5). In two patients, a weaker HG response was also observed during go trials. The HG effect occurred before the estimated SSRT, but did not differ between SS and US conditions. Brain regions critical for stopping should show differential activity between successful and unsuccessful stop-trials in a time-range before the SSRT. Our results are more in line with an attention signal which is reduced or absent in the more frequent, less attention-demanding go-signals (Chikazoe, 2010; Erika-Florence et al., 2014; Swick et al., 2011). The absence of stopping-specific effects in PFC electrodes is consistent with data from PFC lesion patients who had comparable SSRTs to healthy controls (Krämer et al., 2013). One suggestion is that the MFG may facilitate the stopping process by signaling task-relevant stimulus probabilities. In patient S01, an additional Go/No-go task was run with blocks of either 50% or 20% no-go signal probability. In that task, a similar high-gamma increase was observed for no-go trials in the same MFG electrode, which was significantly higher for the 20% vs the 50% conditions (Tzvi et al., under review). In the present study, a post-hoc analysis investigating the correlation between the high-gamma amplitude and the number of go-trials preceding it showed no relationship. Perhaps this MFG site is not involved with directly tracking stimulus probabilities, and the differential stimulus probability effects are due to task-set changes influenced by the stimulus probability.

The notion of inhibition-specific modules in PFC has been questioned recently (Erika-Florence et al., 2014; Mirabella, 2014). Based on fMRI data of different variants of the stop signal task, the authors argued that PFC regions associated with inhibitory functions are part of spatially distributed networks activated when processing infrequent stimuli or learning new tasks (Erika-Florence et al., 2014). Our results support the results in Erika-Florence et al (2014), as the MFG response to the stop-signal could reflect attention towards task relevant sensory input. The effect might be similar to the dlPFC high gamma activity observed in Swann et al. (2012), which was interpreted as related to the task-representation. The activity in their study was observed in response to the task cue, but also to the go-cue in a stop-signal task with a 'maybe stop-go' condition (Swann et al., 2012). However, the observed neural response in this study was more generalized compared to ours, since we only observed the MFG activation following the stop-signal. The results described here as well as in the study by Swann et al. (2012) are consistent with the MFG high gamma activity reflecting attention towards behaviorally relevant signals or retrieval of task goals, which could

generalize to other tasks unrelated to response inhibition (Erika-Florence et al., 2014).

Since this stop-related high-gamma effect in MFG did not distinguish between SS and US, signals related to the decision process may be found in basal ganglia (Schmidt et al., 2013) or possibly motor cortex (van den Wildenberg et al., 2010). Our observations of clear stop related effects in M1 indicate that the decision process possibly occurs in this brain region. Since we did not measure striatal activity we cannot determine if this indeed is the decision process itself, or whether it is a downstream effect from processes in basal ganglia. Regarding the framework proposed by Band and van Boxtel (1999), our results confirmed that M1 is either the site of inhibition, or where the inhibitory process manifests itself (see also Mirabella, 2014). The activations we observed in MFG do not support a role as the inhibition agent. Rather, this signal may be evidence of attentional control, which may potentially be modulating activity of an inhibitory agent in the basal ganglia.

We also observed a later high-gamma increase over more anterior and dorsal PFC sites during stop trials, which occurred after the motor response for US trials. This effect was observed in two out of eight subjects who had electrodes in more frontal and superior sites. For patient S01 this effect was more anterior to the early MFG response, and it was also observed over the left MFG at a slightly more posterior site (patient S07). The late timing indicates that this effect cannot be involved in the stopping process itself. This increase in high-gamma power was enhanced for errors, and may reflect behavioral monitoring. Activity in dorsolateral prefrontal cortex has been consistently linked to top-down control and behavioral adaptation after action errors or response conflicts (Botvinick et al., 2001; Kerns et al., 2004; Marco-Pallares et al., 2008). Notably, the late MFG high gamma response was considerably weaker (in S01) or reversed (in S07) in successful stop-trials. At the same time, patients even showed faster response times after SS trials relative to before. Whereas post-error-slowing in the stop-signal task is a robust finding, behavioral after-effects of SS trials are more variable with many studies reporting no RT change (Verbruggen et al., 2008; Beyer et al., 2014), some reporting an RT increase (Boehler et al., 2010 and some observing an RT decrease (Krämer et al., 2011). A post-inhibition RT decrease with a reduced or absent MFG high gamma effect supports an interpretation in terms of behavioral adaptation. A post-hoc correlation analysis between the amount of post-error slowing and the high-gamma amplitude did not confirm a relationship between the MFG response and behavioral adaptation. However, reaction time changes after successful or unsuccessful stop-trials might reflect not only adaptation and enhanced cognitive control but also simple repetition priming effects (Beyer et al., 2012; Verbruggen et al., 2008). The post-error slowing might thus be a mixture of priming and adaptation effects and not related to the high-gamma MFG response.

Dynamics in the beta band over prefrontal and sensorimotor cortex

Engel & Fries (2010) suggested that beta frequencies might signal the maintenance of the sensorimotor and cognitive set and are involved in the suppression of novel or unexpected external events. The beta rhythm has also been referred to as an idling rhythm (Engel and Fries, 2010; Miller et al., 2012) potentially fulfilling a role in suppressing local cortical activity, while beta desynchronization might enable the transition into an active processing state (Miller et al., 2012).

We observed two different beta power effects. In peri-central sulcus sites, we observed a beta increase for SS, which sometimes coincided with a beta decrease for motor response trials (go and US; see Fig. 2.7A). This is in line with a motor maintenance study in macaques which showed that activity in peri-central sulcus and parietal cortex was organized in a large-scale network characterized by beta band coherence (Brovelli et al., 2004). In the present study, we found changes in beta power in similar peri-central sulcus and superior parietal sites, possibly reflecting different nodes of the sensorimotor network.

We also analyzed changes in beta power specific to stop-trials to test the hypothesis that right IFG beta activity mediates inhibition in a fronto-basal ganglia network involved in stopping (Swann et al., 2009, 2012a). We found beta effects in both left and right IFG or MFG, which resembled results reported by Swann et al (2009; 2012) in rIFG. However, we did not find a difference between SS and US conditions, confirming observations that these beta changes in IFG may be variable across patients (Schall and Godlove, 2012). An explanation for this could be that the stop signal tasks used previously were more complex (Swann et al., 2009, 2012a), possibly causing an increased involvement of the PFC compared to the simpler stop-signal task used in the present study. Another explanation might be that the inter-trial-interval in the study by Swann et al (2009) was not jittered, whereas it was in the present study. A recent MEG study in humans using a cued anti-saccade task observed increased beta power over prefrontal sites when preparing for an anti-saccade compared to a pro-saccade (Hwang et al., 2014). Perhaps the increased predictability of when to be ready for response inhibition is reflected by increased beta band synchronization.

We also found stop-related beta effects in the left PFC, which is not in accord with a strict lateralization of response inhibition to the right PFC (Aron et al., 2014; Swann et al., 2009, 2012a). In agreement with our ECoG findings, a recent study with PFC lesion patients (Krämer et al., 2013) showed that patients with lesions in either left or right PFC had a similar speed of stopping compared to age-matched controls, but increased commission error rate in Nogo-trials. This result can be explained by an attentional control function of the lateral PFC rather than by inhibition implementation (Erika-Florence et al., 2014; Swick et al., 2011).

Conclusions

Our findings argue for a role of monitoring for task-relevant sensory signals and of task performance in sub-regions of the lateral PFC during motor inhibition. The early stop related activity over right and left MFG likely reflects attention-related activity to the behaviorally relevant stop-signals, whereas the late stop-related in rostral PFC activity tracks behavioral performance. Inhibition-related modulation of beta oscillatory activity was found over sensorimotor areas including M1 supporting the notion of a beta-mediated network of motor control.

Chapter 3: The posterior superior temporal gyrus integrates predictive information

Abstract

Context modulates sensory activations. These modulations enhance perceptual and behavioral performance (Holdgraf et al., 2016), and have been hypothesized to reflect a mechanism reducing prediction errors (Friston, 2005). However, the mechanism of when and where these high-level expectations act on sensory processing is unclear. Here, we aim to isolate contextual effects on auditory processing by omitting expected sounds. This approach allows us to infer specific effects of expectations on internally generated responses, in the absence of auditory evoked activity. To investigate this, electrophysiological signals were recorded directly from the superior temporal gyrus (STG) and superior temporal sulcus (STS) in 6 patients with medically refractory epilepsy who were implanted with electrode grids and depth electrodes covering perisylvian cortex centered on the STG, spaced between 3 and 10mm. These signals were recorded while subjects listened to a sequence of syllables in a regular pattern La-La-Ba; La-La Ga. The 'Ba' and 'Ga' syllables were randomly and infrequently omitted from the sequence, enabling us to isolate expectation signals, and also assess whether omission responses were specific to stimulus identity. The prediction literature suggests that omission signals would be maximal in auditory active sites and these would be specific to the stimulus identity. We found a robust high frequency band (HFB, 70-150Hz) response to omissions, which overlapped with only a posterior subset of auditory active electrodes. A classification of the heard syllables using a linear classifier was successful. However, a linear classifier applied to HFB omission activations to omissions was unsuccessful in predicting which stimulus was omitted. This result indicates that this posterior omission HFB activity does not carry information on which stimulus was omitted. We propose that the posterior STG and adjacent posterior STS is central for implementing predictions in the auditory environment, but HFB activations in this region do not reflect stimulus-specific information. The posterior STG is known to integrate incoming auditory signals with other high-level information (Ozker et al, 2017), and omission HFB activations appear to reflect more general mismatch-signaling or salience detection processes (Downar et al, 2000).

Introduction

Expectations influence sensory processing

The notion that the brain uses prior knowledge to make predictions about incoming sensory input has gained considerable traction (Arnal and Giraud, 2012; Friston, 2010, 2009). The idea is that the brain does not process incoming sensory signals in a pure feed-forward manner as previously believed (Serre et al., 2007), but implements cortico-cortical feedback that influences sensory processing in a top-down, hierarchical manner (Lee and Mumford, 2003; Rao and Ballard, 1999). The advantage of a prediction strategy is improved perception and behavior (Anllo-Vento, 1995; Mangun, 1995). On a behavioral level, prior knowledge causes noisy speech to become intelligible. The underlying mechanism for this includes neural changes in auditory processing, as expectations rapidly change auditory perceptive field responses (Holdgraf et al., 2016). Evidence of expectations influencing early sensory processing have also been shown in vision as reductions of the V1 BOLD response to expected gratings (Alink et al., 2010). In audition, expected repetitions of tones also reduce N100 amplitude in MEG (Todorovic et al., 2011).

Prediction

These observations have been explained within a predictive coding framework. Local sensory neurons are hypothesized to be 'error-detection' units (Rao and Ballard, 1999), and prediction errors may then be propagated up the hierarchy (bottom-up) (Friston, 2005). According to Friston & Kiebel (2009), the brain operates to 'explain-away' signals from lower levels of processing, providing an account for reduced responses to expected stimuli. However, a discrepancy in the literature is apparent when on the one hand predictions are proposed to reduce neural responses lower in the sensory hierarchy (Friston, 2010), yet predictable stimuli are more easily decoded from V1 voxels despite smaller BOLD responses (Kok et al., 2012). This suggests that predictions may not simply reduce neural activity in sensory processing areas, but perhaps facilitate processing the expected stimulus by providing enhanced stimulus-specific information (Kok et al., 2012). These findings allude to a more complex mechanism of prediction than proposed by predictive coding, and important aspects of the underlying neural mechanism remain to be elucidated.

Investigating auditory context processing through omissions

Studies investigating predictions generally manipulate stimulus predictability or embed stimuli in noise, and the resultant auditory activity is a confluence of bottom-up sensory processing, and expectation modulations. Here, we aimed to isolate

expectation effects on auditory cortex by examining the neural signals to omissions of expected sounds. Omissions of expected sounds have been shown to elicit ERP responses ~100ms in EEG proposed to be generated in auditory cortex (Bendixen et al., 2014; Sanmiguel et al., 2013). In the visual domain, omission signals in V1 have been shown to contain stimulus specific information, since the omitted stimulus can be decoded from V1 voxels using fMRI, and has been interpreted as an activation of a stimulus template (Kok et al., 2014). In auditory cortex, omitted speech sounds embedded in words can also be recovered from HFB activity in STG. These omitted sections were replaced by noise, and HFB reconstructions matched the perceptual experience of the subject (Leonard et al, 2016). HFB activity has been shown to drive the fMRI BOLD response, and correlates with neural firing, providing a link between different methods (Niessing et al., 2005; Ray and Maunsell, 2011). Therefore, we utilized the high spatial- and temporal resolution of ECoG to 1) isolate potential prediction-related HFB activations to auditory omissions in human auditory cortex, 2) define the spatiotemporal dynamics of these activations, 3) determine whether this HFB activation carries stimulus-specific information.

Methods

Participants and experimental setup

A total of 6 subjects (1 female, mean age 43, range between 31 and 69) participated in the current study (see Table 3.1, appendix A, for further demographic information). These subjects were recruited from a patient group with medically refractory epilepsy undergoing neurosurgical treatment, and had subdural electrodes implanted for clinical purposes. These patients were tested during clinical monitoring in their hospital bed, and typically remained implanted for a duration of 4-10 days. All patients gave their informed consent according to the declaration of Helsinki, and an additional verbal consent was given prior to each testing session. Patients were recruited from different sites, including Albany Medical Center (AB, n=5) and UC Irvine (IR, n=1). Institutional Review Boards from each individual site and UC Berkeley approved the experimental procedures.

Electrophysiological signals were recorded using either a g.Tec g.HIamp system and digitally sampled at 9.6 kHz (AB), a Nihon Kohden system with a 128-channel JE-120A amplifier at a sampling rate of 5kHz or 10kHz (IR). Electrode grids used were spaced between 3-10mm, with platinum iridium electrodes, and were manufactured by AdTech or PMT. Depth electrodes were spaced 5mm apart, and were manufactured by AdTech. Reconstructions of electrode placement were made using pre-operative T1 structural MRI scans, and post-operative CT scans. Average brain projections were done with the use of the Fieldtrip matlab toolbox (Oostenveld et al., 2011). Timing of stimuli was recorded in analog channels by splitting the speaker signal from the experimental computer to the recording system. Responses in the form of finger taps were recorded using a microphone plugged into an analog channel (IR), or using a response button (AB). Analog channels were recorded at 5kHz or higher.

Experimental Task

To ensure high predictability of the stimuli, we played a repetition of the pattern 'La-La-Ba La-La-Ga', using syllable stimuli created and shared by the Shannon lab at USC. We chose to use syllables as stimuli to ensure robust auditory activations in the STG. 'Ba' and 'Ga' were chosen, since these syllables have been previously shown to be decodable from this region (Chang et al, 2010). We used a third syllable 'La' as a filler, to set up a temporal expectation of the 'Ba' or 'Ga' to be played. To ensure that the subject was attentive to the sounds, the subject was instructed to respond to a 'Ta', which we randomly introduced in place of the 'Ba' or 'Ga' as a target stimulus 5% of the time. Since the task is very repetitive, we chose a target stimulus close to the other stimuli, to prevent the subject from ignoring the stimuli and simply rely on

bottom-up salience of a target stimulus. Finally, the relevant task manipulation was the omission of either 'Ba' or 'Ga'. The syllables lasted 410 ms each, and the ISI within a 'La-La-Ba' triplet was fixed to 200ms, whereas the ISI between triplets was 400ms (Irvine) or 200ms (Albany). We recorded between 3 and 6 blocks in each subject, with each block including 16 omission trials, 8 target trials, and 68 'Ba' and 'Ga' presentations respectively, and lasted about 4 minutes. The experiment was coded using E-Prime 2.0 software (Psychology Software Tools, Pittsburgh, PA), or BCI2000 (Schalk et al., 2004) for the Albany recordings.

Preprocessing

The data was analyzed using custom-written scripts and the MNE package in python (Gramfort et al., 2013). All data was down-sampled to 1kHz or 1.2kHz (AB only) after a 500Hz low-pass filter, corrected for DC shifts, band-pass filtered between 0.5Hz and 220Hz, and notch-filtered to remove line-noise at 60Hz, 120Hz and 180Hz, using a FIR filter from the MNE Python toolbox (Gramfort et al., 2013). AB data was filtered at 1Hz to 190Hz due to intermittent high-frequency machine noise above this frequency. All channels were re-referenced to a common average, which sometimes was calculated per individual grid if noise patterns were different (surface electrodes), or were bipolar referenced (depth electrodes). Timing of stimuli and responses was extracted from the analog channels. Omission onsets were calculated by subtracting the onsets of the previous two stimuli ('La-La'), and added to the onset of last stimulus (second 'La').

Electrophysiological analysis

Spectral power was calculated using Hilbert transform after band-pass filtering between 70-150Hz. Statistical evaluations were done on the single trial analytic amplitudes. We employed a non-parametric clustering algorithm (Oostenveld et al, 2008) on a time-window of 0-500ms comparing single trial analytic amplitudes in omission trials to a baseline of 200ms to 50ms before the stimulus was expected. The power percent change was calculated relative to an average of a baseline taken 200ms to 50ms before stimulus onset. Time-course plots were made using the Seaborn python visualization package, with error bars signifying a 68% confidence interval bootstrapped across trials.

For binary classification, we used a linear support vector machine classifier from the scikit-learn python toolbox. Prediction accuracies were obtained using a 10-fold cross-validation. The first classification approach involved an electrode selection based on how good each electrode classifies Ba vs Ga (actual sounds). The purpose of this classification approach is to test if auditory sites distinguishing between the heard sounds also distinguish which stimulus was omitted. A separate classifier for each electrode was applied on its HFB data from 0-500ms relative to

stimulus onset. If an electrode had a prediction accuracy of more than 60% based on hearing the spoken sounds, it was included in omission classification. For omission classification, this selection of electrodes' HFB data from 0-500ms relative to omission 'onset' was included in a single classifier. Both training and testing were done on omission trials. A second classification approach included features of omission HFB data that survived a statistical threshold compared to baseline. This specifically tested whether HFB increases to omissions carried information on which stimulus was omitted. The statistical threshold consisted of applying non-parametric permutation clustering on individual electrodes in a time-window of 0-500ms, comparing omission HFB to baseline. HFB activity for significant clusters was subsequently used as features to classify which stimulus was omitted. Linear classifiers were also applied to individual electrodes on omission data (HFB 0-500ms) for visualization purposes only, in order to compare single electrode performance between heard and omitted 'Ba' and 'Ga' (Fig. 2.4).

Results

Behavioral results

The behavioral data show that subjects responded to targets with average reaction times ranging between 438ms and 643ms, and an average across subjects of 552ms ± 156ms (Table 3.2, appendix A). The hit rate across subjects is 90%, with the lowest individual hit rate at 81%. Subject AB71 had a larger number of false alarms (43 trials) compared to the other subjects, i.e. button presses to 'Ba' or 'Ga'.

High Frequency Band activations in auditory regions to syllables

The HFB task activations in auditory regions for individual subjects are shown in Figures 3.1 and 3.2. Figure 3.1 shows two subjects with high-density grids (3mm) covering the STG. Panels A and C show that auditory activations to syllables evoke a robust HFB activation in the STG. This auditory activation typically onsets <100ms, as can be seen in the time-courses plotted in panels B and D (blue and red traces). These activations were significant compared to baseline with clusters in 87 electrodes for AB62, and 98 electrodes for AB81 (cluster permutation, 0-500ms, $p<0.05$). Additional subjects show similar patterns, as can be seen in Figure 3.2A and 2C. Here, AB71 showed significant HFB activations compared to baseline in 31 electrodes, AB78 in 15, AB79 in 46 electrodes (Topographies in Fig. 3.1 and 3.2 show data in significant electrodes only). In addition, we also found robust auditory activations in the superior temporal sulcus (Figure 3.2, subject IR39).

High-gamma activations in auditory regions to omissions

Responses to omissions are shown in Figure 3.1 and 3.2 (light-colored red and blue traces). As evident in Fig. 3.1A, we found HFB activations to omissions, which predominantly occur in posterior subsets of auditory active electrodes. Example anterior electrodes with clear auditory activations show smaller, or no increase in HFB power for omissions (Fig. 3.2C, Fig. 1B, D), whereas posterior electrodes show robust power increases in response to omissions, which peak between 200-400ms (Fig 3.1B, D; Fig. 3.2D). Interestingly, in subject AB62 (Fig. 3.1B, second plot) the HFB power seems to deviate from baseline at 0ms, the cluster in this specific electrode showing a significant difference compared to baseline, indeed includes all time-points within the tested time-window, starting at 0ms ($p<0.002$). However, this early HFB increase was not observed in lateral STG in other subjects.

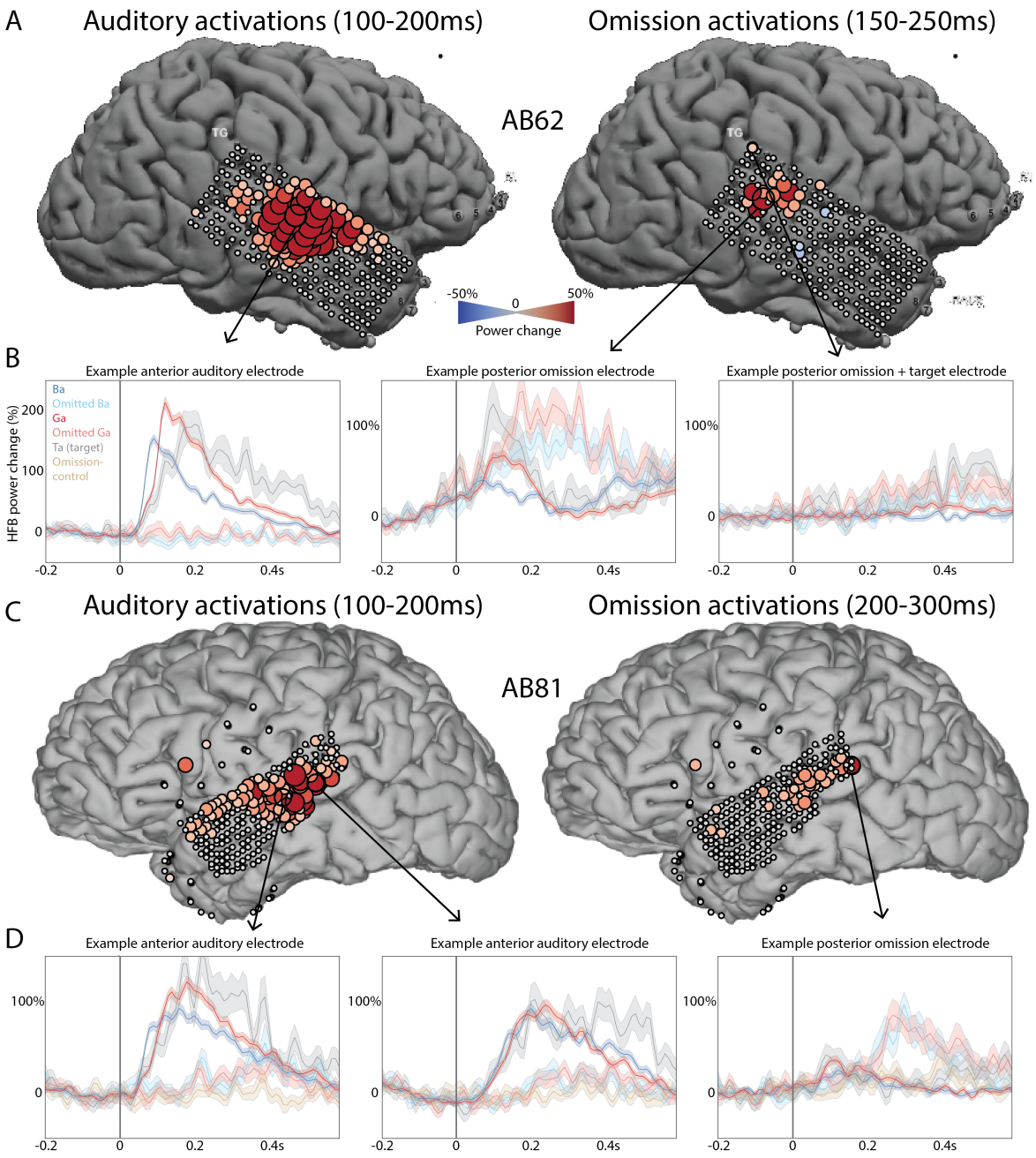

Figure 3.1 HFB activation patterns for spoken and omitted sounds for two high-density (3mm) grid subjects. A) Topography of HFB activations for subject AB62. HFB power is averaged for (omitted) 'Ba' and 'Ga' presentations, over a time-window of 100-200ms (left) and 150-250ms (right). B) three example electrodes showing 1) auditory but no omission activations, 2) auditory and omission activations, and 3) omission and target, but no auditory activations. Stimulus onset is at 0ms, and traces are HFB responses to 'Ba' (darkblue), 'Ga' (darkred), omitted 'Ba' (lightblue), omitted 'Ga' (lightred), 'Ta' (gray) and an omission control (tan) C) Topography of HFB activations for subject AB81. HFB power is averaged for (omitted) 'Ba' and 'Ga' presentations, over a time-window of 100-200ms (left) and 200-300ms (right) D) Three example electrodes for showing both auditory and omission activations.

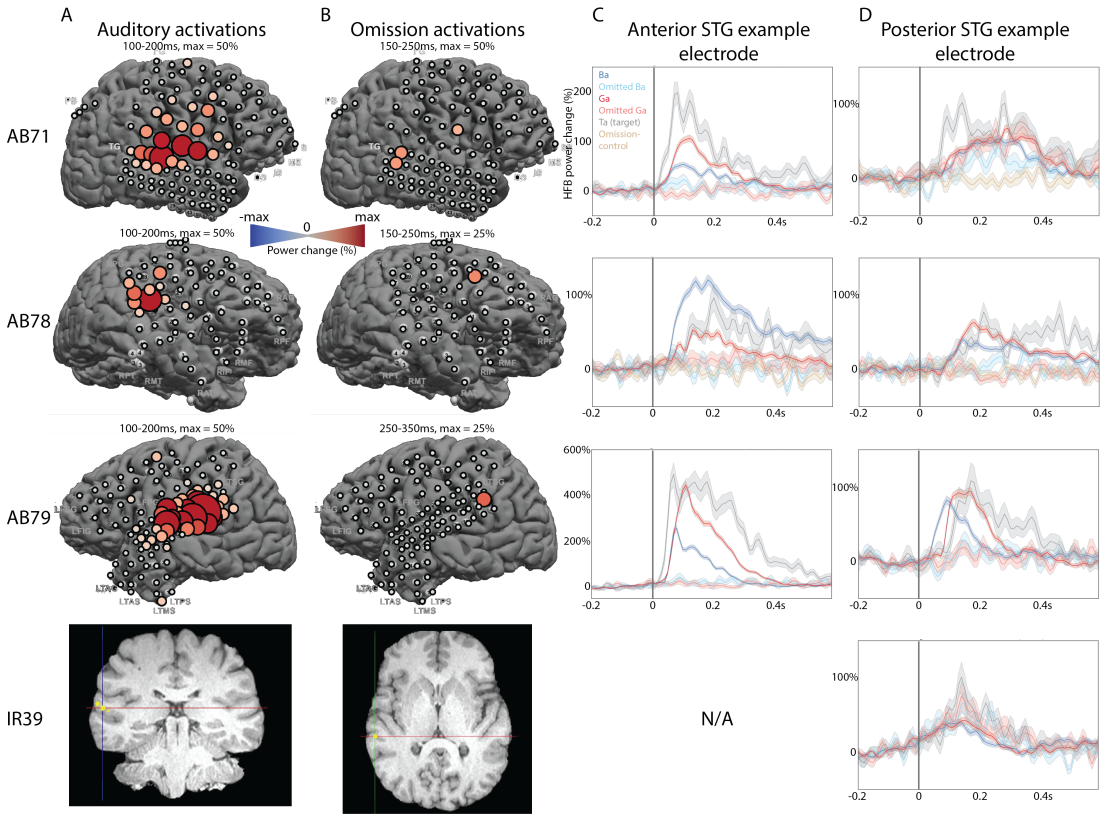

Figure 3.2 Auditory and omission HFB activations in additional subjects. A) Topography of significant auditory HFB power change. Specific time-window and scale are shown above each plot. Subject IR39 only shows the electrode location. B) Topography of significant omission HFB power change C) Example auditory electrodes in anterior STG. Stimulus onset is at 0ms, and traces are HFB responses to 'Ba' (darkblue), 'Ga' (darkred), omitted 'Ba' (lightblue), omitted 'Ga' (lightred), 'Ta' (gray) and an omission control (tan) D) Example auditory electrodes in posterior STG (or STS for IR39)

Figure 3.2 also shows omission activations in subjects AB71 (3 electrodes, cluster permutation, 0-500ms, $p<0.05$), AB79 (5 electrodes) and IR39 (1 electrode). Note that these omission responses are not limited to the lateral surface of the superior temporal gyrus, as subject IR39 shows a similar response in a depth electrode in the temporal lobe, more specifically in STS. In some cases the omission activation is similarly sized or larger compared to the auditory activations (Fig 3.1B&D). Some electrodes showing omission activations are unique in that they show both omission and target activations, but not auditory activations (Fig 3.1B, third example electrode). Subject AB78 shows auditory activations, but no significant omission responses in any of the auditory active electrodes. With the auditory activations being located on the edge of grid, it is possible that we are missing coverage of the relevant posterior STG region in this subject. The anterior versus posterior character of auditory evoked- and omission responses is further visualized in Figure 3.3, showing the locations of all electrodes with significant auditory HFB activations

only (blue), omission activations only (orange), or significant activations in both conditions (magenta). Note that some electrodes in inferior frontal gyrus also show auditory- and omission HFB activations in subjects AB71, AB78 and AB81.

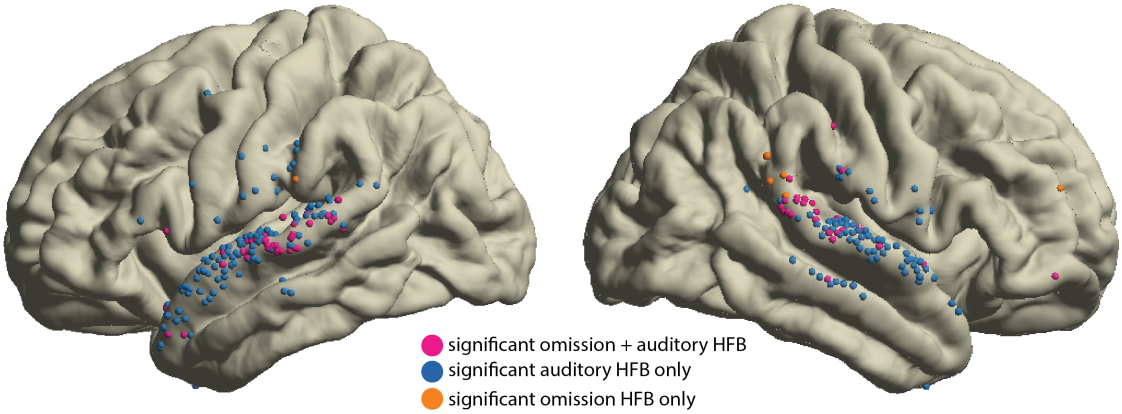

Figure 3.3 Overview of results showing omission responses in posterior auditory active sites, including electrodes from subjects AB62, AB78, AB79, AB81 projected onto the average MNI brain. Pink colored electrodes are electrodes with both significant auditory and omission HFB power increase versus baseline, blue colored electrodes signify electrodes with significant auditory HFB power increases only, whereas orange colored electrodes only show significant omission HFB power increases (0-500ms, $p<0.05$ cluster permutation)

Decoding analysis using auditory HFB activations to sounds and omissions

Decoding analysis of spoken sounds was successful for heard syllables at the single electrode level, with prediction accuracies >80% in some electrodes (see Fig. 3.4A). To specifically test whether auditory sites distinguishing between 'Ba' and 'Ga' can also distinguish which of these two syllables were omitted, we employed a classifier on a time-window of 0-500ms, including all electrodes with predictions >60% for heard 'Ba' and 'Ga'. This classifier's performance remained at chance level, meaning what stimulus was omitted could not be decoded from HFB activity in syllable selective sites in STG with this approach. In addition, we tested if HFB increases to omissions in STG were predictive of which stimulus was omitted. Electrodes and time-windows were selected based on HFB power comparisons to baseline using the cluster permutation method within electrodes in a time-window of 0-500ms. All significant clusters were subsequently included as features to classify which stimulus was omitted. This approach also remained at chance level. For illustration purposes only, prediction accuracies for classifiers applied to single electrode HFB between 0-500ms for omissions are shown in 3.4B alongside the single electrode classification of heard syllables.

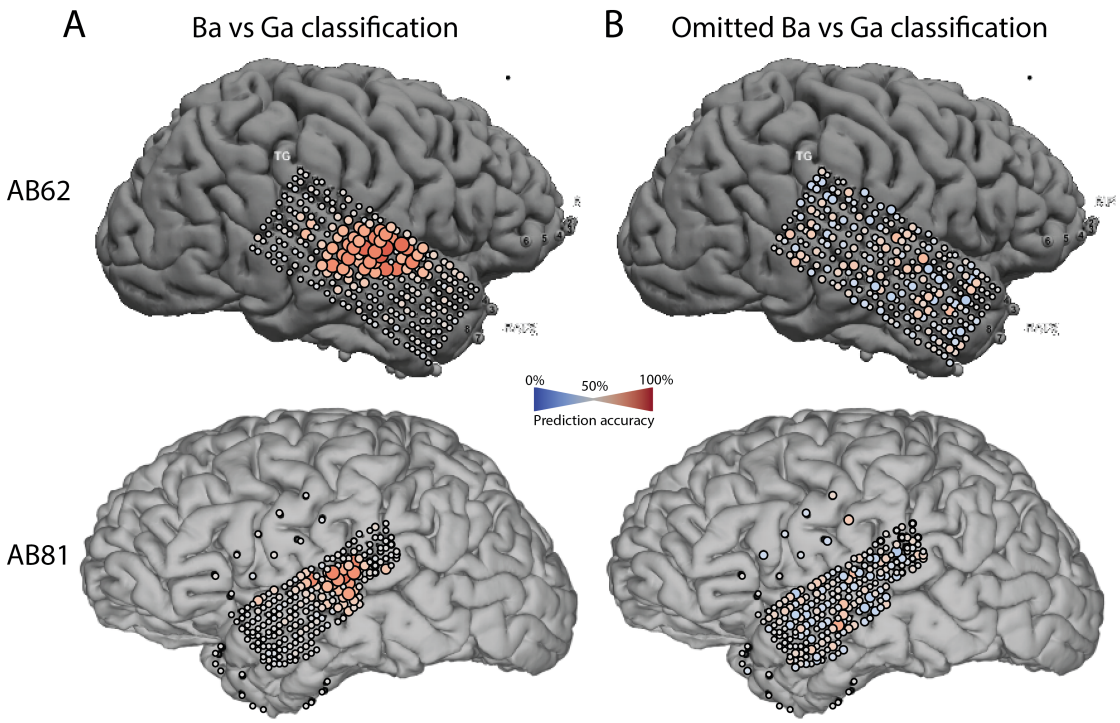

Figure 3.4 Single electrode classification prediction accuracies for classifying heard Ba vs Ga (panel A) and omitted Ba vs Ga (panel B). Top plots show subject AB62, bottom plots show subject AB81. This is for illustration purposes only, and deviates from the final classification described in the text with respect to omission decoding.

Discussion

We used intracranial recordings to investigate expectation effects on auditory cortex. We aimed to isolate endogenous HFB processes related to contextual processing by examining omissions of expected sounds. We found a posterior subset of auditory active electrodes in the STG that showed HFB power increases to omissions (Figure 3.1-3). However, information on which stimulus is omitted does not seem to be encoded in these HFB power increases (Figure 3.4).

Posterior STG shows activations to omissions of expected sounds

We found HFB power increases to omissions of expected speech sounds. These activations were observed in all subjects except AB78, which may be due to limited coverage over posterior auditory areas in STG. Because we used spoken sounds as stimuli, we could uniquely map out auditory processing regions in STG that may not respond to simpler stimuli, such as tones used in other studies including mismatch designs (Dürschmid et al., 2016; Edwards et al., 2005). The most notable observation about the auditory and omission activation patterns was that omission activations were observed in a posterior subset of auditory-active electrodes in the STG (Figs 3.1-3). This is contrary to that expected of a prediction error signal according to theories of hierarchical mechanisms of predictive coding. Here, a prediction error is hypothesized to be produced and propagated along the hierarchy of sensory processing (Bastos et al., 2012; Friston, 2010). However, our HFB omission activation selectively occurs in only a subset of auditory responsive sites, whereas HFB power to omissions remains at baseline in other electrodes strongly responding to speech sounds.

The anterior versus posterior separation of the omission activations we observed may be related to anatomical separations of the auditory processing stream, as our findings overlap with recent findings from intracranial recordings. A study by Ozker et al (Ozker et al., 2017) shows that noisy speech in the presence of contextual cues differentially affects posterior and anterior STG. Here, HFB responses to speech in posterior STG remains unaffected by added noise with context, whereas auditory activations degraded in anterior STG, suggesting a multi-modal integration role for pSTG. In our task contextual information did not arise from a different modality, suggesting that this region may implement contextual processing both within and across modalities. Specific damage to the pSTG and angular gyrus has been associated with a specific auditory short-term memory deficit (Gazzaniga et al., 2002; Markowitsch et al., 1999). Perhaps the pSTG is supporting auditory short-term memory critical for recognizing patterns and signaling deviations. An anterior-posterior division has also been reported in right STG for consonant compared to dissonant cords processing (Foo et al., 2016). This division has also been reported on in spoken sentences, with the posterior STG

responding mostly to onsets of sentences and emphases on syllables, whereas the anterior STG remains active throughout the sentence, suggesting a specialization of temporal or salience processing in the posterior STG, compared to feature processing in anterior STG (Hamilton et al., 2017). Context therefore seems to have a restorative effect on auditory HFB responses in pSTG, and contextual information affects auditory HFB responses differentially following an anterior-posterior division. Posterior and anterior auditory cortex has also previously been suggested to be divided into a dorsal and ventral stream (Bizley and Cohen, 2013). Combined, these studies and our data point to a specialized role of pSTG within the auditory stream related to implementation of contextual information.

HFB omission activations are temporally persistent

Another characteristic of the HFB power increases to omissions shown here is that they span several hundreds of milliseconds. For some subjects significant activations occur in latencies as early as 0ms to 100ms. This is most notable in subject AB62 (Fig. 3.1B), in which the posterior electrode shows HFB deviating from baseline as early as 0ms to both sounds and omissions. In contrast, an anterior electrode shown in Fig. 3.1B shows auditory activations deviating from baseline at ~50ms (Picton et al., 1974b), following more standard bottom-up auditory cortex processing time-scales. However, the largest amplitudes are reached at latencies >100ms, extending to 200-400ms.

These omission signals can be evaluated according to two functional roles with differential temporal profiles: 1) Activations could signify preparatory processes as part of a predictive process, and would therefore be expected to occur early (<100ms) 2) activations could also be an omission response, perhaps signifying surprise in the form of a mismatch, or prediction error (Wacongne et al., 2011), and/or auditory saliency detection (Downar, Crawley, Mikulis, & Davis, 2000). Given our results, we may be seeing both processes at work in the same region. First, HFB activity may be elevated in the anticipation of a stimulus, which subsequently turns into a surprise signal once the expected stimulus fails to appear. Anticipatory neural firing has been observed in rat auditory cortex in a task manipulating temporal expectations (Jaramillo and Zador, 2011), and we may be seeing a neural correlate of that rodent finding in HFB in AB62 and IR39. The degree of attentiveness by the subject may have influenced whether this HFB anticipatory increase can be observed, explaining why it is not evident in other subjects. However, HFB activation >100ms are robust across all subjects with sufficient STG coverage. Thus, this omission response points most strongly to a surprise or mismatch signal.

No evidence for stimulus specific information in omission HFB

We found electrodes in pSTG encoding phonemic information, evident from different amplitudes and time-courses distinguishing between heard syllables (Figs. 3.1 and 3.2). Decoding which syllable was heard was robust (Fig. 3.4). To test if a stimulus template was activated during omissions of expected sounds, we applied a classifier to HFB power time-courses in omission trials, only including electrodes with reliable prediction accuracies for which sound was heard. This classification approach proved unsuccessful. After evaluating the HFB activations to omissions it became evident that not all auditory active sites exhibited omission HFB power increases. We therefore re-ran classification of which stimulus was omitted on electrodes with significant HFB increases, specifically including only those time-points within a window of 0-500ms that were included in the significant clusters. This classification attempt also remained at chance level, indicating that the omission HFB response in STG does not distinguish between which stimulus was predicted and omitted.

Based on previous decoding and encoding approaches, the HFB seemed to be the most likely signal to contain information on stimulus-specific predictions (Chang et al., 2010; Flinker et al., 2011; Holdgraf et al., 2016; Martin et al., 2014; Pasley et al., 2012). However, it could be that stimulus-specific information is not carried by activity in the HFB. For example, the gamma (30-70Hz) and beta (15-30Hz) frequency bands have been previously implicated in prediction processes (Arnal and Giraud, 2012; Bastos et al., 2012). Another explanation could be that such template-specific activations are only occurring in primary auditory cortex which we could not access (Kok et al., 2014, 2012). Finally, it could be that the omission of a sound is more salient than the omission of a *specific* sound. Given the specific saliency or temporal characteristics of auditory processing in this region, we speculate that the omission response observed here may be related primarily to when the stimulus is expected, and is a temporal prediction violation.

Contextual processing and the posterior STG

A large body of work assigns a multitude of functions to the posterior STG including speech processing, face processing, audiovisual integration, motion processing and theory of mind (as reviewed by Hein & Knight, 2008). This region is also prominently featured in the ventral attention network, which comprises pSTG, the temporo-parietal junction (TPJ), inferior frontal gyrus (IFG), insula and cingulate cortex (Downar et al., 2002). This network has been interpreted to identify salient events, and to re-orient attention (Corbetta and Shulman, 2002; Downar et al., 2000). This is not surprising, as a deviation from the expectation of what is coming next is necessary to classify a stimulus as novel, or salient. Contributions from the TPJ specifically, and its relation to the P300 ERP, have been re-evaluated to be

involved primarily in contextual updating (Geng and Vossel, 2013). Contextual updating would update the prediction for the next trial, based on the outcome of the current. The full cycle of the prediction process therefore follows a time-course that extends beyond early sensory processing. Our data may provide clues to the recruitment of auditory regions and their temporal dynamics at different stages of this process. Similar to Downar et al, we find differential omission activation patterns in the posterior STG/TPJ region and IFG (Figs. 3.1-3). Some anterior and posterior STG sites are involved specifically in auditory and omission processing, whereas a more posterior site does not show auditory activations, and responds more strongly to targets over omissions (Figure 3.1B, third plot). This is in accordance with modality general TPJ activations, whereas posterior STG is specific to auditory novelty (Downar et al., 2002). The posterior STG may comprise the first node in the network for the detection of salient auditory events. In addition, some sites in IFG are also active to omissions (Fig. 3.1-3). The P3a response has been connected to the ventral attention network, and has been observed in an equivalent EEG study of the task used here (see Chapter 4). Given the apparent non-specific, prolonged nature of the HFB omission activation, local neural activity underlying this activation might be involved in binding anticipatory processes with the auditory mismatch process and the salience detection network.

Conclusions

We show that omissions of expected sounds elicit a robust HFB increase in auditory active regions in posterior STG. We demonstrated that omission HFB is only present in a subset of posterior STG auditory active electrodes, following a similar division of anterior vs posterior auditory processing in STG as shown in recent papers (Hamilton et al., 2017; Ozker et al., 2017). In some sites omission HFB activity deviated from baseline before 100ms. Contrary to predictions from the literature, a classification analysis applied to this HFB increase in posterior STG was unsuccessful in predicting which stimulus was omitted, suggesting that the observed omission HFB activation does not carry stimulus-specific information. Finally, this response is different from that seen in the TPJ, which was shown to respond to omissions and targets, but not to sounds generally.

Chapter 4: Posterior superior temporal cortex contributions to auditory omission-induced ERP's – a combined EEG and ECoG study

Abstract

Brain responses to omissions of expected stimuli provide a powerful tool to study endogenous neural processes to prediction and mismatch signaling in the absence of stimulus-evoked activity. Several omission event-related potentials (ERP's) have been observed to omissions of expected sounds. These include negative deflections linked to N100 (N1), the mismatch negativity (MMN) and the attention-related N200 (N2) ERP, all believed to be generated in auditory cortices. In addition, longer latency positive ERP's such as the P3a (novelty), or the P3b (target-detection) are observed depending on task-set.

Here, we performed a combined EEG and ECoG study on infrequent omissions of spoken sounds presented in a highly regular pattern. We show that omissions elicit both a negativity (peak latency at 46ms) followed by a P3a response both with classic frontal topographies in the scalp EEG. We then investigated cortical sources of omission-related components by recording the same task in two patients undergoing intracranial monitoring for clinical purposes. Here, we observed the classic auditory P50 and N1 to spoken sounds, as well as an omission negativity (N2) in the superior temporal gyrus (STG) peaking at 200ms. This omission negativity was located posterior to the N1 topography in STG. Overall, we establish in EEG that P3a ERP's can be observed in response to an omission that is not task-relevant but unexpected, which is preceded by a negativity in the first 100ms after the omitted sound was expected. We also find a possible source of scalp omission negativities intracranially in the STG, which may contribute to the omission negativities observed in the EEG.

Introduction

The brain continuously anticipates events in the external world, and the signaling of unexpected events is vital to re-orient attention and, if necessary, adjust behavior. Omissions of expected stimuli are a unique way of investigating endogenous neural processes related to anticipatory and mismatch detection processes, as bottom-up sensory activations are absent. A variety of event related potentials (ERP's) have been observed to omissions of expected sounds in EEG (Picton et al., 1974a; Simson, 1976; Snyder and Hillyard, 1976), intracranial EEG (Alain et al., 1989; Hughes et al., 2001; Rosburg et al., 2005), and in event-related fields (ERF) in MEG (Raij et al., 1997; Todorovic et al., 2011). Raij et al (1997) showed that negative deflections in the ERF related to omissions can be traced to auditory regions in temporal cortex, peaking at a latency of 145-195ms after the onset of the omitted expected stimulus that. Some studies also describe endogenous auditory-like potentials to omissions such as the N1 (SanMiguel et al., 2013b), or the P50 (Bendixen et al., 2009). These early auditory potential imitations may be related to mental imagery of the omitted stimulus (Bendixen, SanMiguel, & Schröger, 2012; Janata, 2001).

A well-known ERP called the mismatch negativity (MMN) has also been implicated in signaling an omission (Bendixen et al., 2012), and has been proposed as a potential prediction-error signature (Wacongne et al., 2012). This ERP is generally seen when auditory stimuli deviate from a pattern at a latency of 100-250ms, and is insensitive to attention manipulations. It is proposed that the MMN is generated as part of an automatic deviant detection mechanism that occurs locally in auditory cortex, where a memory trace of the pattern is held (Naatanen et al., 2007). Recordings in macaque show that an MMN is observed only in supragranular layers of A1, suggesting a local process independent of thalamocortical inputs (Javitt et al., 1994). Lesions of the temporal and frontal cortices in humans also show impairments of the MMN (Alain et al., 1998). The MMN has been observed with respect with mismatches of timing of stimuli, including stimuli that appeared earlier than expected (Ford and Hillyard, 1981; Naatanen et al., 1993), and omissions (Nordby et al., 1994; Yabe et al., 1998). However, the omission MMN is also sensitive to temporal spacing of the stimuli in a sequence, i.e. the MMN only occurs when the stimulus onset asynchrony (SOA) is smaller than ~170ms (Yabe et al., 1998). This suggests that the omission MMN is bound to a temporal window of integration, and does not occur when the stimulus interval is larger than 200ms. However, some omission responses in auditory cortex occur with stimulus intervals greater than 200ms, i.e. 500ms or 1s, and also are enhanced with attention (Raij et al., 1997). This suggests that either negative omission ERP's ~100-250ms measured in auditory cortex are not necessarily an MMN response, or the MMN response to

omissions in sequences at longer time-scales may behave differently and have a different temporal profile.

Other ERP's that have been related to mismatch or novelty processes are the N2b, generally occurring at 250ms to 300ms (Folstein and Petten, 2008a; Naatanen and Picton, 1986), and the P3a, a positivity generally peaking at 300 to 350ms for rare stimuli in the auditory domain (Comerchero and Polich, 1999; Johnson, 1993; Polich, 2007). The N2 category encompasses three main ERP's: the N2a, generally equated to the MMN, the N2b, which has been related to novelty processes and has a frontal-central topography, and the N2c, occurring more posterior and occuring with target detection (Folstein and Petten, 2008a). Originally, an omission-N2 was given its own category (Naatanen and Picton, 1986), but since it has been suggested it may overlap with the N2a or N2b categories (Raij et al., 1997). The N2b often occurs together with the P3a (Snyder and Hillyard, 1976), and it has been suggested that they are two aspects of the same process (Naatanen and Picton, 1986). The P3a, like the N2b, is known for its occurrence in response to salient or novel stimuli and its fronto-central topography in EEG. The P3a is different from a target-detection P3b, which has a more parietal topography (Polich, 2007). Lesions in either lateral frontal cortex and temporo-parietal cortex reduce both P3a and P3b amplitudes (Knight and Scabini, 1998), and it has been suggested that the origin of the P300 is distributed across association cortex and may have multiple sub-components (Johnson, 1993; Kam et al., 2016). The P3a has also been observed in response to non-target omissions of visual stimuli (Czigler et al., 2006), and a P3b occurs to target-omissions (Picton et al., 1974a).

Here we describe omission ERP's in a task recorded in healthy subjects using EEG, as well as intracranial recordings in auditory cortex in surgical patients. We evaluate the occurrence of the above-mentioned ERP's, and compare them across the two methods.

Methods

Participants and experimental setup

EEG: Nineteen healthy participants were recruited for the EEG study (6 male), with a mean age of 21 (range of 18-27), one participant was left-handed. Subjects were recruited on the UC Berkeley campus through course credit or were monetarily compensated. Subjects gave their informed consent according to the declaration of Helsinki. Electrophysiological signals were measured from the scalp using a 64 active electrode Biosemi system. An average of left and right mastoid reference channels was used as a reference. A total of three external electrodes were used to measure eye-movements.

Intracranial EEG: Two subjects undergoing neurosurgical treatment for medically refractory epilepsy participated in the study, while recording electrophysiological signals from intracranial electrodes. The patients were tested during clinical monitoring in the hospital room. All patients gave their informed consent according to the declaration of Helsinki. For intracranial patients an additional verbal consent was given prior to each testing session. Intracranial patients were recruited from Albany Medical Center, Institutional Review Boards from both Albany Medical Center and UC Berkeley approved the experimental procedures. Electrophysiological signals were recorded using either a g.Tec g.HIamp system and digitally sampled at 9.6 kHz. High-density grids were used with platinum iridium electrodes spaced 3mm apart (center-to-center), and were manufactured by PMT. Reconstructions of electrode placement were made using pre-operative T1 structural MRI scans, and post-operative CT scans. Timing of stimuli were recorded in the BCI2000 recording and presentation software (Schalk et al., 2004).

Experimental Task

The same task was used in both the EEG and intracranial EEG studies, and is also described in Chapter 3. To ensure high predictability of the stimuli, we played a repetition of the pattern 'La-La-Ba La-La-Ga', using syllable stimuli created by the Shannon lab at USC. We chose to use syllables as stimuli to ensure robust auditory activations in the STG. 'Ba' and 'Ga' were chosen, since these syllables have been shown to be decodable from this region (Chang et al, 2010). Temporal expectations for the 'Ba' and 'Ga' sounds were set up by using a third syllable 'La' as a filler. To ensure that the subject was attentive to the sounds, the subject was instructed to respond to a 'Ta', which we randomly introduced in place of the 'Ba' or 'Ga' as a target stimulus 5% of the time. Since the task is very repetitive, we chose a target stimulus close to the other stimuli, to prevent the subject from ignoring the stimuli and simply rely on bottom-up salience of a target stimulus. Finally, the relevant task manipulation was the omission of either 'Ba' or 'Ga'. The syllables lasted 410 ms

each, and the ISI was fixed to 200ms. We recorded between 6 blocks in each subject, with each block including 16 omission trials, 8 target trials, and 68 'Ba' or 'Ga' presentations respectively, and lasted about 4 minutes. The experiment was coded using E-Prime 2.0 software for the EEG experiment (Psychology Software Tools, Pittsburgh, PA), or BCI2000 (Schalk et al., 2004) for the Albany intracranial recordings.

Preprocessing

Intracranial EEG: Data was down-sampled to 1.2kHz after a 600Hz low-pass filter, corrected for DC shifts, band-pass filtered between 1Hz and 10Hz, using a FIR filter from the MNE Python toolbox (Gramfort et al., 2013). Finally the data was down-sampled to 100Hz. Channels were re-referenced to the common average across all electrodes.

EEG: Data was recorded at 1024Hz sampling rate, and referenced to contacts on the left and right mastoids. Preprocessing and analyses were done in matlab using the Fieldtrip toolbox (Oostenveld et al., 2011). The data was low-pass filtered at 30Hz, excessive jumps and muscle activity in the data were removed, and eye-movement artifacts were removed using ICA. A final visual inspection of summary statistics (variance, z-score, min/max values) was done to remove problematic channels or trials. The data was subsequently down-sampled to 256 Hz. For visualization purposes, the EEG data was base-lined by subtracting the average of a window of -200 to -100ms.

Statistical evaluation

For statistical evaluations of condition differences the cluster-permutation implemented in the Fieldtrip (EEG) or MNE (intracranial EEG) toolboxes was used (Gramfort et al., 2013; Maris and Oostenveld, 2007; Oostenveld et al., 2011). To evaluate early negative ERP's we used an a priori time-window of 0-300ms, and compared omissions to non-target stimuli ('Ba' and 'Ga'). For the P3 evaluations we used an a priori time-window of 200-500ms, comparing omissions to non-target stimuli ('Ba' and 'Ga'), and comparing target ('Ta') to non-target stimuli. Further characterization of the non-invasive ERP's latency and amplitude involved selecting a peak electrode (Fz and Pz), and determining these measures for each subject using the maximum value in the 200-500ms time-window. A similar within-subject characterization was done for the intracranial recording.

Results

Behavioral results

The behavioral results for healthy subjects show an average reaction time to targets of 570ms ± 67ms (mean and sd), and a hit rate of 72% ± 13%. This can be compared to a hit rate of 98% and average reaction time of 661ms ± 224ms (mean and sd) in intracranial subject AB62, and a hit rate of 85% and average reaction time of 563ms ± 193ms for subject AB81. Typically, intracranial subjects are more variable in their behavior, and slower than healthy subjects, explaining the relative slow reaction times of subject AB62. However, in this case the intracranial subject far exceeds the average behavioral performance of the healthy EEG subjects.

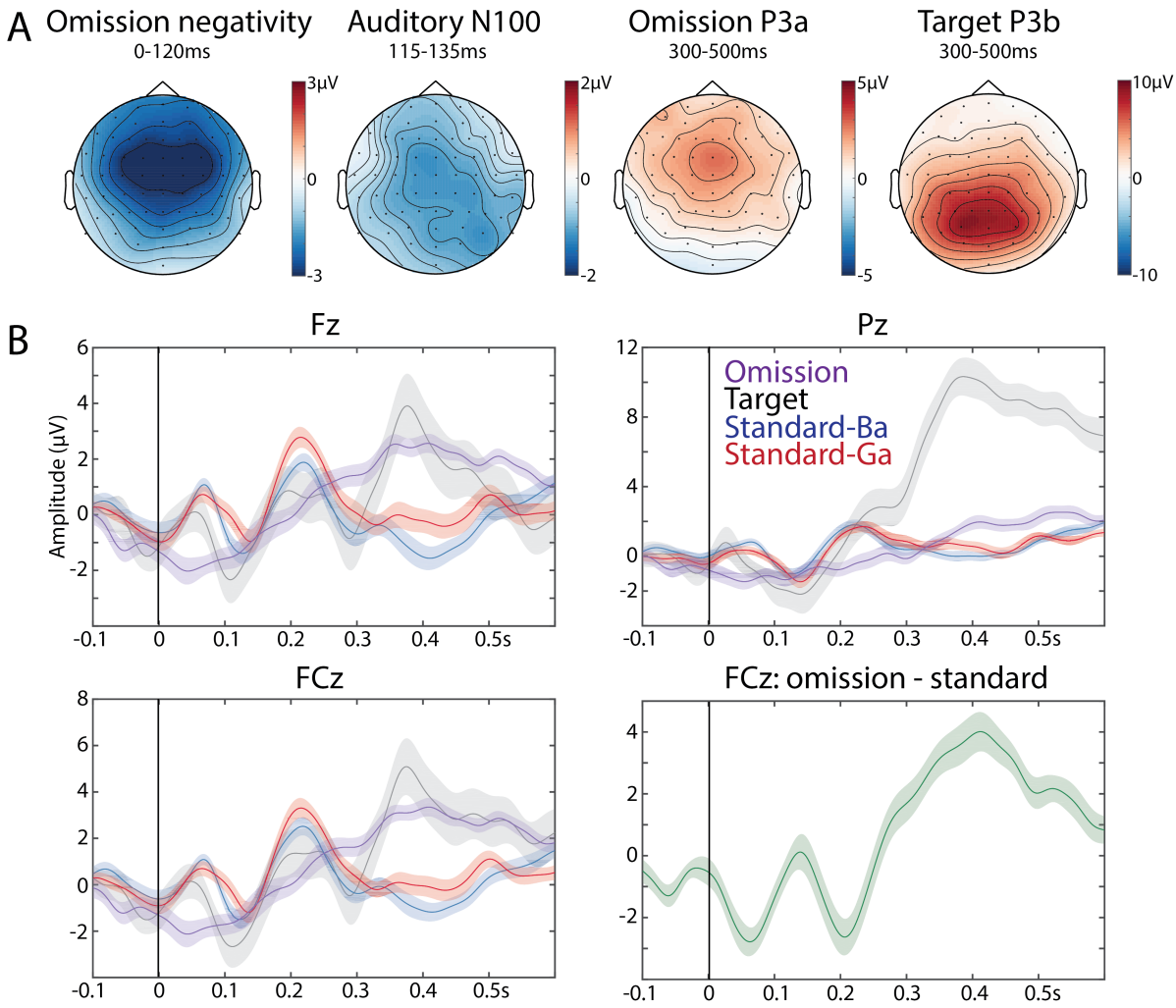

Figure 4.1 EEG ERP results. A) shows the topographies for the omission negativity, auditory N1, P3a and P3b ERP's. B) ERP traces for select Fz, FCz and Pz. A difference plot in FCz of omissions and standards is shown in the lower right (green trace). Stimulus onset is at 0ms, and traces are responses to 'Ba' (darkblue), 'Ga' (darkred), omissions (purple), 'Ta' (gray).

ERP's to omissions and target stimuli in EEG

A negative deflection can be seen in the first 200ms with a fronto-central topography, peaking at ~40ms as measured from the average omission trace in FCz (Fig. 4-1). A difference wave of omission minus non-targets shows two negative peaks, one at peaking at ~60ms, and one at ~200ms, followed by a P3a response (Fig. 4.1B, lower right). A cluster-analysis comparison of omissions to non-target stimuli shows a significant difference at 2ms to 120ms (cluster $p<0.006$), although individual negative peaks between 0 and 200ms for omissions are at 130ms ± 78ms in FCz. As can be seen in Figure 4.1, omissions also elicit a robust P300 response with a frontal distribution reminiscent of the P3a (272ms to 500ms, cluster $p < 0.001$). This ERP has a peak amplitude of 4.4μV ± 2.8μV (mean ± sd) and a peak latency of 368 ± 121ms as measured in FCz. Target stimuli elicit a parietally located P3b response (299ms to 500ms, cluster $p<0.001$), which has a peak amplitude of 11.5μV ± 6.2μV and a peak latency of 412 ± 118ms as measured in Pz. The target P3 is typically larger (paired t-test, $p<1e-5$) than the novelty P3, and occurs a with a longer latency, though the latency difference was not significant (paired t-test, $p = 0.0533$).

ERP's to omissions and target stimuli in intracranial EEG

In the intracranial data we investigated potential contributions to omission ERP's in auditory cortex, and more specifically STG. Figure 4.2 shows the topography of auditory and omission ERP's in two subject with extensive coverage of the superior temporal gyrus. The topography for the auditory-evoked P50 and N1 in STG can be seen in panels B and D ($p<0.05$, 50-90ms P50/90-130ms N1, one-sided cluster permutation test). The P50 overlaps with the N1, but the center of gravity is more posterior in AB62. The omission negativity encompasses the P50 and N1 activation regions, but also includes electrodes more posterior to both the P50 and N1 topographies. Omission negativity peaks at 200ms (AB62), and 300ms (AB81), after the expected onset of the omitted sound ($p<0.05$, two-sided cluster permutation test). The time-courses on the right in Fig. 4.2 show omission negativity being present in electrodes showing P50 and N1 (Fig. 4.2B right plot), but larger amplitudes are reached in more posterior electrodes, where P50 and N1 amplitudes are significantly reduced. In sum, the omission negativity presents with partially overlapping, but distinct topographies compared to the auditory evoked potentials.

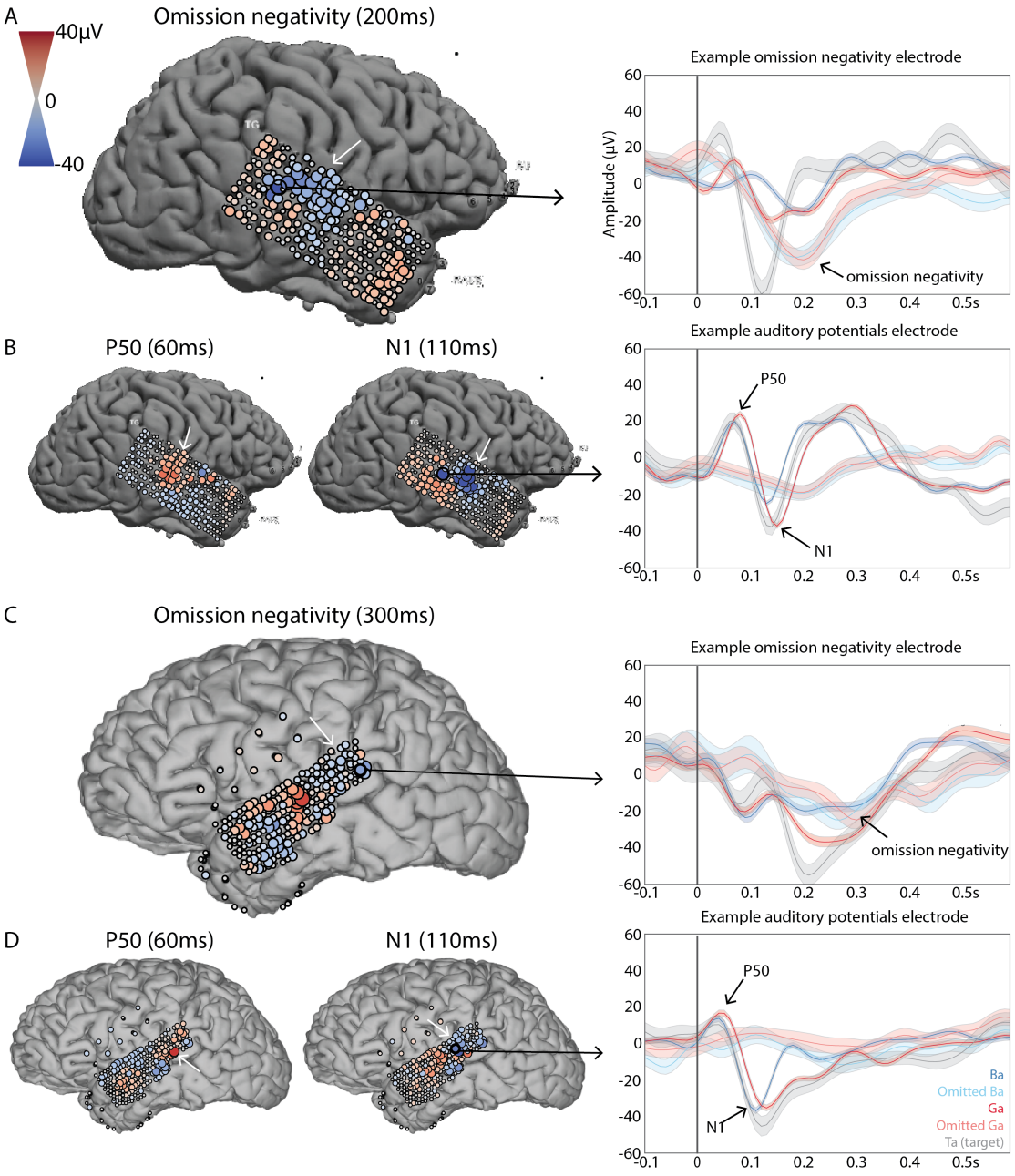

Figure 4.2 Intracranial ERP topographies (left) and example electrodes (right). Stimulus onset is at 0ms, and traces are HFB responses to 'Ba' (darkblue), 'Ga' (darkred), omitted 'Ba' (lightblue), omitted 'Ga' (lightred), 'Ta' (gray). A) and C) show the omission negativity for subject AB62 and AB81 respectively. B) and D) show the P50 and N1 auditory ERP's for subject AB62 and AB81 respectively.

Discussion

In this chapter we presented a comparative study of omission-related ERP's in EEG and ECoG measured from auditory cortex. We show robust P3a and P3b responses to omissions and target stimuli respectively. In both EEG and ECoG we show an omission negativity. This presents fronto-centrally in EEG, and was measured directly from STG in ECoG. A comparison with auditory evoked ERP's in STG shows that the omission negativity overlaps in topography with P50 and N1, but also includes sites posterior to these observed auditory ERP's.

Omission-related negativity observed in EEG

We observed a prominent ERP effect manifesting as a fronto-central negativity at 40-200ms after the expected onset of the omitted sound. This response overlaps temporally with other studies describing omission negativities (Raij et al., 1997; SanMiguel et al., 2013a; Yabe et al., 1998). This negativity seems to occur a bit too early to be interpreted as a classical MMN (Naatanen et al., 2007), though the MMN may not occur with the relatively long SOA used in our experiment (Yabe et al., 1998). Rather, the observed omission negativity seems to overlap more with N1-like responses described by SanMiguel et al (2013) and Todorovic et al (2011), but is the opposite of an early P50-like positivity to omissions described by Bendixen et al (2009). The task designs in both these studies are very different from the study described here, making it difficult to compare. An important aspect of the negativity we observe is that is reaches significance at a very early latency of 2ms, and is more likely related to a process anticipating an expected sound, rather than being an omission response. Indeed, this negativity may even start before the expected onset, as the signal seems to show a downward slope in the baseline prior to the timing of an omission.

Auditory evoked and Omission-negativity in STG

We observed robust P50 and N1 auditory evoked ERP's in STG. The topography of the P50 concentrates more posteriorly compared to the N1 topography. In addition, we found an omission-negativity in STG, confirming source modeling of a similar omission-related negativity observed in an MEG study by Raij et al (1997). This negativity peaks at ~200-300ms after the onset of the omitted sound, and overlaps with auditory evoked ERP topographies, albeit extending more posteriorly as well. This effect adds to existing literature showing omission ERP's (Hughes et al., 2001), and deviant sound MMN (Edwards et al., 2005; Rosburg et al., 2005) recorded intracranially from supratemporal cortex. The MMN reported by Edwards et al (2005) show an MMN anterior to the N1 topography in STG, whereas we observe a negativity posterior to the N1. This could either mean that the omission negativity we observe is not an MMN, or it can be explained by the different nature of the

'deviant', potentially producing an MMN in a different part of the auditory stream. Indeed, an anterior-posterior division of auditory processing has been suggested (Bizley and Cohen, 2013), and a deviation of pitch may be signaled in a different region of auditory cortex compared to temporal deviations.

Comparison of omission negativity observed in EEG and ECoG

In both EEG and ECoG we observed a negativity at early latencies (<250ms). However, there are some clear differences in the temporal characteristics. In the EEG, the negativity shows up very early (peak latency at 40-60ms), and might be initiated prior to the onset of the omitted sound. In contrast, the intracranial negativity measured in STG starts after the expected onset (~100ms), and peaks at 200-300ms. A potential explanation for this is that the EEG negativity is a composite of negativities from multiple sources, which may include the STG source. This source in STG could be interpreted as an auditory contribution to an N2b. The presence of a P3a to omission in the EEG makes it likely that the STG negativity could be related to an N2b process. This N2b-P3a complex was observed in the EEG difference wave shown in Figure 4.1B. Note that this difference wave is not an ideal comparison, as one condition elicits auditory evoked potentials whereas these are absent in omissions. Perhaps the STG source could be interpreted as an MMN. Despite previous studies showing that SOA's longer than 170ms do not elicit omission MMN's, we speculate that perhaps shorter interval MMN's are generated in Heschl's gyrus, whereas longer intervals might be signaled in higher order auditory cortex in STG. This would mean that perhaps longer time-scales are being integrated higher in the auditory hierarchy. The dipoles generated in Heschl's gyrus and STG would be partially orthogonal to each other, and show up with differential topographies in EEG/MEG. We therefore do not exclude the possibility that the STG negativity is a temporal MMN. Finally, the STG negativity may be an omission process not directly related to either the MMN or N2b. The posterior STG is known for being part of the ventral network (Downar et al., 2000), and the negativity observed could be evidence of an auditory cortex contribution to saliency detection.

EEG shows robust P3a to omissions and P3b to target sounds

The P300 ERP has been extensively studied and widely reported on in the literature (as reviewed by Polich, 2007). In our experiment we observe the classic P3b to target sounds, an ERP understood as being related with target detection and contextual updating processes, with a typical parietal topography. That we observe a P3a response to omissions indicates that the omission in our experiment was a salient, attention capturing event. This may include the recruitment of attentional processes, either for the evaluation of the current event or for a contextual update (Polich, 2007). A P3 response to omissions has been reported in omission detection

tasks. Specifically, the observation of a P3b response in an omission detection task was important evidence for the endogenous cognitive nature of the P3b, as opposed to a stimulus-evoked ERP (Picton et al., 1974a). The P3a is sometimes also observed in response to omissions (Czigler et al., 2006; Raij et al., 1997), but not always (Yabe et al., 1998). Our results further establish the occurrence of P3a to omissions of spoken sounds.

Conclusions

We observed an early omission negativity fronto-centrally in EEG, which may be a composite of anticipatory and mismatch processes. We also found an omission negativity directly recorded in STG, posterior to and overlapping with the auditory N1 topography. This STG negativity may be related to either a 'long latency' MMN, or it could be an auditory contribution to the N2b supported by the presence of a subsequent P3a, or it may be an omission process on its own. This intracranial negativity resembles the omission negativity described by Raij et al (1997), and confirms their source modeling results locating the ERP in STG. We also observe a P3b to target sounds, as well as a P3a to omissions, further contributing to the omission P3a literature. Overall, our results show a clear source of omission signaling in auditory cortex.

Chapter 5: Discussion

In this thesis we have investigated two important aspects of the perception-action cycle. We started with investigating inhibitory motor control, a function exemplifying the importance of fast-acting integration of information between perception and action. We showed that HFB activations are inhibited in M1 for successful inhibitions, and we presented stop-related and behavioral monitoring HFB activations in MFG. Next we investigated how the brain might implement prediction to aid perception and behavior. Specifically, we examined expectation effects on auditory cortex by omitting expected sounds. We found that a posterior subset of auditory active sites in STG show HFB activations to omissions. However, this HFB activation did not carry information on which stimulus was omitted. In addition, we have shown that omissions evoke negative potential deflections at 0-300ms both intracranially as well as in EEG, as well as a saliency P3a response in EEG.

Inhibitory motor control and frontal cortex

The first part of this thesis concerns frontal contributions to response inhibition. Within the perception-action cycle, the frontal cortex plays a crucial role in the temporal organization and (pre-) adaption of goal-directed behavior (Fuster, 2013). For response inhibition a fast integration of new information pertaining to the task is necessary to appropriately respond to our ever-changing environment. To understand how the frontal cortex contributes to response inhibition we employed electrocorticography, a method with a unique spatio-temporal resolution.

Distinct stopping implementation and -evaluation processes in Frontal cortex

In Chapter 2 we found that the stopping process acts on M1 as evidenced by a well-known beta rebound (Swann et al., 2009; Zhang et al., 2008), as well as greatly reduced or absent HFB activations for successful stops. In MFG, we describe HFB activations that seem to be related to two distinct processes. The first HFB effect peaks around the SSRT, and shows no difference between successful and unsuccessful stops (Fig. 2.4-5). Usually response inhibition studies analyze data based on differences between successful and unsuccessful stops (Neubert et al., 2013), assuming that the stop-related activations must be different if the outcome is different. However, the original horse-race model of response inhibition describes the stopping process as an *independent process* (Logan et al., 1984), and stopping-related brain activity does not have to be indicative of the outcome. This HFB activation could evidence of this stopping process. The second stopping-related HFB activation we found in MFG occurs later, i.e. after the response in unsuccessful stops,

and is stronger for errors (Fig. 2.6). This activation is likely related to behavioral monitoring and evaluation. Recent research has replicated these two kinds of stopping-general, as well as stop-error preference HFB activations in other regions, e.g. IFG and anterior insula (Bartoli et al., 2017).

Frontal roles in stopping: IFG vs MFG

A notable difference between the response inhibition literature and our results is that we did not find clear HFB activations in right IFG. This area has been implicated as a frontal stopping locus (Aron et al., 2004), with evidence provided from fMRI, TMS and lesion studies [as reviewed by](as reviewed by Aron, Durston, et al. 2007). Instead we found robust HFB activations in MFG, which has been shown before in fMRI (Garavan et al., 1999). Other intracranial studies have shown involvement of the IFG and MFG in stopping as well. Swann et al (2009) for example showed a beta increase that was stronger for successful stops in IFG. Although we did replicate this beta increase in IFG, we did not find a difference between successful and unsuccessful stops. Other intracranial studies on response inhibition involving analysis of HFB show activations in this band in MFG as well as IFG and anterior insula (Bartoli et al., 2017; Swann et al., 2012b). This has been interpreted as the MFG, or dorsolateral PFC, implementing and retrieving the task goal, whereas IFG implements stopping (Swann et al., 2012b). Indeed, the authors show that the dlPFC HFB activations precede IFG activity. Bartoli et al (2017) also studied stopping related activations, but limited their analyses to IFG and anterior insula. Interestingly, their activation patterns of stopping-general HFB activity after the stop-signal, but before the SSRT, as well as failure-preferring post-SSRT activity resemble the two activation patterns we found in MFG. Previous findings using fMRI also show distinct inhibition and feedback processes in IFG (Hirose et al., 2009).

There are a number of factors that could explain differences between these intracranial studies. First, it could be caused by inter-individual differences, as well as sub-sampling of the cortical space. It is known that HFB activity can be independent across electrodes spaced 4mm apart in auditory cortex (Flinker et al., 2011). If this is true for PFC as well, we could have missed critical IFG sites. Another difference is the nature of the stop-signal, which is a color-change of a visual stimulus in our task, whereas other intracranial studies employed an auditory stop-stimulus (Bartoli et al., 2017; Swann et al., 2009, 2012b). The auditory cortex is known to have a strong anatomical connection to the IFG via the Arcuate Fasciculus (REF), so there might be modality-specific differences of IFG involvement. Finally, the frontal cortex may be implementing different stop-related functions that are distributed across this region, concentrated in IFG and MFG. This could explain localization of these functions to specific regions, as well as characteristic stop-related activations being measured across different regions with a more fine-

grained approach such as intracranial EEG. It is therefore not a question whether right IFG implements stopping itself, or implements attentional control (Neubert et al., 2013), but how sub-networks distributed across the frontal cortex *not limited to IFG* differentially support the signaling of the stop stimulus, implement task-set, modulate attentional resources, as well as implement behavioral monitoring. Future research should take into account the possibility of multiple processes being supported by specific networks, as well as include a wide search space within frontal cortex for stopping-related processes.

Auditory prediction: a specialized role for posterior STG?

The second part of this thesis examines auditory prediction processes through omissions of expected sounds. The unique spatiotemporal resolution of ECoG allowed us to evaluate effects with respect to their timing relative to when a sound was expected, as well as pinpoint predictive processes to specific regions within auditory cortex. In addition, recording the same task in healthy individuals using non-invasive EEG provided a comparison between methods, yielding additional information aiding the interpretation of intracranially recorded potentials and HFB activations.

Integrating HFB activity with intra- and extra-cranial ERP's: a saliency story?

In **Chapter 3** we showed that omissions elicit a HFB responses in a posterior subset of auditory active electrodes in STG. Although this effect was significant <100ms in some subjects (Figs. 3.1&3.2), alluding to anticipation processes, the most robust effect across subjects was a HFB increase peaking at 200-400ms. In **Chapter 4** a negative deflection of the ERP was shown in STG, overlapping the region in which the omission HFB activations are observed (Figs. 3.1&4.2). This negative ERP was evident in EEG, specifically in a difference wave in FCz (Fig. 4.1B). The comparison of omissions with standard sounds may not be the optimal contrast, as auditory evoked potentials may not be easily distinguished from omission-induced responses. We did observe an earlier negativity with a fronto-central topography (Fig. 4.1), which may be related to N1-like (Bendixen et al., 2012) or MMN processes in primary auditory cortex, as these processes are not clearly discernable in lateral STG ECoG. The occurrence of a P3a component to omissions in EEG provides us with an important clue for interpreting the intracranial negativity and HFB activations in STG. The P3a is associated with novelty or salience detection (Polich, 2007), and although the STG responses may not directly contribute to the P3a generation, they may be signatures of cortical processes leading up to it. The P3a is known to be preceded by a negative component called the N2b (Folstein and Petten, 2008b; Naatanen and Picton, 1986), and the negativity observed in pSTG may be the auditory generator of this component.

Both auditory processing literature as well as the literature concerning cognitive-related functions, are converging on an anterior-posterior division of STG. On the one hand it has been suggested that the auditory system may be divided into two parallel streams of processing, a dorsal and a ventral stream (Bizley and Cohen, 2013; Dewitt and Rauschecker, 2013). Both monkey and human studies have shown that anterior STG is involved in vocalization and speech processing, whereas posterior STG is involved with self-produced speech and sound location (as reviewed by Dewitt & Rauschecker 2013). A recent human intracranial study showed a similar division, i.e. anterior HFB activity seems to be involved with speech processing throughout a sentence, whereas posterior STG becomes active to onsets of sentences and emphasized syllables (Hamilton et al. 2017). The posterior STG has also been implicated with multiple cognitive functions, among which the ventral attention network, which also includes the TPJ and IFG (Corbetta and Shulman, 2002; Downar et al., 2000). A single-case lesion of the posterior STG and angular gyrus showed an impaired short-term auditory memory (Markowitsch et al., 1999). The posterior STG has also been shown to integrate contextual information, restoring HFB activity to noisy speech, whereas anterior STG has significantly reduced HFB activity (Ozker et al., 2017). The question is: how can we integrate the dorsal auditory pathway with contextual, attention and short-term memory functions of the posterior STG?

Here, our data may provide a crucial link between contextual processing, as we see activations in this auditory region *in the absence of sound*, and the specificity of auditory features processed in this region. The nature of expectations represented in posterior STG may be primarily non-speech related, and rather encode temporal or other physical sound features, perhaps explaining why detailed information on which syllable was omitted could not be recovered. The posterior STG may also be a specialized auditory context integration hub, explaining why we see omission HFB activations in this region and not in anterior STG. This explanation also fits with posterior STG being involved with auditory short-term memory, as well as salience detection. Our data support both of these functions ascribed to pSTG, as omission activations necessarily require a tracking of auditory patterns, and signaling a deviation of this pattern is a necessary first step of salience detection.

Predictive suppression versus facilitation

The next question is how our data on omissions of expected sounds may provide clues into the neural mechanism of predictive strategies implemented by the brain. As described in Chapter 1, two dominant views on predictive process are predictive coding (Friston, 2005; Rao and Ballard, 1999) and hierarchical Bayesian inference (Lee and Mumford, 2003). The first hypothesizes a suppression of predicted

information, and emphasizes signaling of prediction errors, whereas the second describes a mechanism facilitating information consistent with higher-level predictions (Olshausen, 2014). Our omission HFB activation and N2 ERP in pSTG could be interpreted as a prediction error signal. The question remains why more anterior auditory sites do not show a similar error signal? The notion of the pSTG as an auditory context integration hub might explain this localization of the omission response, but it seems to contradict the strong proposed hierarchical nature of predictive models. Speech comprehension, a function assigned to anterior STG, improves with prediction, and has a restorative effect on auditory HFB activations (Holdgraf et al., 2016; Leonard et al., 2016). An explanation may be that prediction errors are not encoded in the ERP or HFB, or error signals in anterior auditory regions are too subtle to break the noise floor. But perhaps prediction errors are not as robust as predictive coding seems to suggest, and an inference mechanism of facilitation and selective suppression can explain this selective mismatch signal to omissions in pSTG.

In order to understand how hierarchical predictive processes act on auditory processing, we need to improve our understanding of the hierarchical organization of auditory cortex. How to reconcile the dual auditory stream with models of hierarchical predictive processes, and a seemingly specialized role for contextual processing in pSTG remains an open question. Our results confirm expectations influencing auditory regions in pSTG, but further research of contextual effects on auditory processing along the anterior-posterior axis is necessary.

Human electrophysiology methodologies

It is evident that measuring electric fields of the brain provide us with important clues for how the brain functions. The non-invasive EEG is useful, as it is a relatively low-cost method, and can be applied easily to large numbers of healthy subjects. Results across subjects are relatively uniform, and easily averaged. Disadvantages of the method include poor spatial resolution and attenuation of higher temporal frequencies due to the skull acting as a temporal and spatial filter (Nunez and Srinivasan, 2006). Further, the EEG signal is often not sufficient to do single-trial analysis precluding within subject statistics. The field of intracranial EEG research allows us to measure the electric fields of the brain at their source. For obvious reasons this type of recordings can only be done in neurosurgical patients with brain tumors and/or suffering from epilepsy. Alterations to the brain due to condition or medication use might influence our results, and it is important to validate intracranial results with other methods in healthy subjects. Nonetheless, intracranial recordings have given us unique insights into the spatiotemporal dynamics of perceptual processing and cognitive functioning. Comparative studies

such as described in this thesis are of vital importance, as they provide us with important clues that can be applied to non-invasive studies of the brain.

Concluding remarks

In this thesis we provide crucial evidence for the understanding of inhibitory motor control and auditory prediction, provided by a combination of ECoG and EEG recordings. We show that HFB activity patterns in MFG are reflective of distinct processes of stopping implementation, as well as behavioral monitoring. Combined with findings from other groups we suggest that inhibitory control network contributions from PFC are distributed and multi-faceted, meaning that sub-regions of PFC implement multiple stop-related functions, and these stop-related functions are supported across PFC.

A study of omissions of expected sounds showed HFB activations in a posterior subset of auditory-active sites in STG. Decoding attempts on which sound was omitted were unsuccessful, both when applied to HFB activity from syllable-selective electrodes, as well as to omission HFB activations specifically. In the same region we observed a negative ERP peaking at 200-300ms. This negative peak was only discernable in the EEG in a difference wave calculated relative to standard sounds in FCz. An early omission negativity (peak latency 40-60ms) was observed in FCz, which may reflect anticipatory or N1-like processes. This effect was not observed in lateral STG, but may originate in primary auditory cortex.

The presence of a P3a ERP in EEG provides an important clue into evaluating the intracranial HFB and ERP responses to omissions. The posterior STG has been implicated with contextual and salience processing (Corbetta and Shulman, 2002; Downar et al., 2000; Hein and Knight, 2008; Ozker et al., 2017). Our results provide evidence of a process integrating expectations with incoming auditory signals, that may act as an auditory node in the ventral attention network. The observed negativity in pSTG may be an auditory contribution to the N2b ERP often observed together with a P3a.

Our results confirm that omission-related activity can be found in auditory cortex (Arnal and Giraud, 2012). However, the spatial specificity of omission responses to a posterior subset of auditory active electrodes was, to our knowledge, not known. Also, contrary to what may be expected based on previous findings (Kok et al., 2014), these signal did not carry information on which stimulus was omitted. Omission-processing may be a function specific to a dorsal auditory processing stream (Bizley and Cohen, 2013; Dewitt and Rauschecker, 2013), explaining its posterior location, and why it does not seem to encode stimulus-specific information.

This thesis contributes to a large body of work showing that context influences sensory processing. It also emphasizes the notion that no brain area can

be evaluated on its own, and should be understood relative to its place in the dynamical system of distributed networks supporting brain functioning.

References

Alain, C., Richer, F., Achim, A., Saint Hilaire, J.-M., 1989. Human intracerebral potentials associated with target , novel , and omitted auditory stimuli. Brain Topogr. 1, 237–245. doi:10.1007/BF01129601

Alain, C., Woods, D.L., Knight, R.T., 1998. A distributed cortical network for auditory sensory memory in humans. Brain Res. 812, 23–37.

Alink, A., Schwiedrzik, C.M., Kohler, A., Singer, W., Muckli, L., 2010. Stimulus predictability reduces responses in primary visual cortex. J. Neurosci. 30, 2960–2966. doi:10.1523/JNEUROSCI.3730-10.2010

Anllo-Vento, L., 1995. Shifting attention in visual space: the effects of peripheral cueing on brain cortical potentials. Int. J. Neurosci. 80, 353–370.

Arnal, L.H., Giraud, A.-L., 2012. Cortical oscillations and sensory predictions. Trends Cogn. Sci. 16, 390–398. doi:10.1016/j.tics.2012.05.003

Aron, A.R., 2011. From reactive to proactive and selective control: developing a richer model for stopping inappropriate responses. Biol. Psychiatry 69, e55-68. doi:10.1016/j.biopsych.2010.07.024

Aron, A.R., Behrens, T.E., Smith, S., Frank, M.J., Poldrack, R. a, 2007a. Triangulating a cognitive control network using diffusion-weighted magnetic resonance imaging (MRI) and functional MRI. J. Neurosci. 27, 3743–52. doi:10.1523/JNEUROSCI.0519-07.2007

Aron, A.R., Durston, S., Eagle, D.M., Logan, G.D., Stinear, C.M., Stuphorn, V., 2007b. Converging evidence for a fronto-basal-ganglia network for inhibitory control of action and cognition. J. Neurosci. 27, 11860–4. doi:10.1523/JNEUROSCI.3644-07.2007

Aron, A.R., Robbins, T.W., Poldrack, R. a, 2004. Inhibition and the right inferior frontal cortex. Trends Cogn. Sci. 8, 170–7. doi:10.1016/j.tics.2004.02.010

Aron, A.R., Robbins, T.W., Poldrack, R. a., 2014. Inhibition and the right inferior frontal cortex: one decade on. Trends Cogn. Sci. 1–9. doi:10.1016/j.tics.2013.12.003

Aron, A.R., Verbruggen, F., 2008. Stop the Presses; Dissociating a selective from a global mechanism for stopping. Psychol. Sci. 19, 1146–1153.

Babiloni, C., Del Percio, C., Vecchio, F., Sebastiano, F., Di Gennaro, G., Quarato, P.P.,

Morace, R., Pavone, L., Soricelli, A., Noce, G., Esposito, V., Rossini, P.M., Gallese, V., Mirabella, G., 2016. Alpha, beta and gamma electrocorticographic rhythms in somatosensory, motor, premotor and prefrontal cortical areas differ in movement execution and observation in humans. Clin. Neurophysiol. 127, 641–654. doi:10.1016/j.clinph.2015.04.068

Ball, T., Kern, M., Mutschler, I., Aertsen, A., Schulze-Bonhage, A., 2009. Signal quality of simultaneously recorded invasive and non-invasive EEG. Neuroimage 46, 708–716. doi:10.1016/j.neuroimage.2009.02.028

Band, G.P.H., Boxtel, G.J.M. van, 1999. Inhibitory motor control in stop paradigms : review and reinterpretation of neural mechanisms. Acta Psychol. (Amst). 101, 179–211.

Bartoli, E., Aron, A.R., Tandon, N., 2017. Topography and Timing of Activity in Right Inferior Frontal Cortex and Anterior Insula for Stopping Movement. Hum. Brain Mapp. 0, 1–15. doi:10.1002/hbm.23835

Bastos, A.M., Usrey, W.M., Adams, R. a, Mangun, G.R., Fries, P., Friston, K.J., 2012. Canonical microcircuits for predictive coding. Neuron 76, 695–711. doi:10.1016/j.neuron.2012.10.038

Bendixen, A., SanMiguel, I., Schröger, E., 2012. Early electrophysiological indicators for predictive processing in audition: A review. Int. J. Psychophysiol. 83, 120–131. doi:10.1016/j.ijpsycho.2011.08.003

Bendixen, A., Scharinger, M., Strauß, A., Obleser, J., 2014. Prediction in the service of comprehension: Modulated early brain responses to omitted speech segments. Cortex 53, 9–26. doi:10.1016/j.cortex.2014.01.001

Bendixen, A., Schroger, E., Winkler, I., 2009. I Heard That Coming: Event-Related Potential Evidence for Stimulus-Driven Prediction in the Auditory System. J. Neurosci. 29, 8447–8451. doi:10.1523/JNEUROSCI.1493-09.2009

Benjamini, Y., Hochberg, Y., 1995. Controlling the False Discovery Rate: a Practical and Powerful Approach to Multiple Testing. J. R. Stat. Soc. 57, 289–300.

Berger, H., 1929. Uber das Elektrenkephalogramm des Menschen. Arch. Psychiatr. Nervenkr. 87, 527–570.

Beyer, F., Münte, T.F., Fischer, J., Krämer, U.M., 2012. Neural aftereffects of errors in a stop-signal task. Neuropsychologia 50, 3304–12. doi:10.1016/j.neuropsychologia.2012.10.007

Binder, J.R., Frost, J.A., Hammeke, T.A., Bellgowan, P.S.., Springer, J.A., Kaufman, J.N., Possing, E.T., 2000. Human Temporal Lobe Activation by Speech and Nonspeech Sounds. Cereb. Cortex 10, 512–528.

Bizley, J.K., Cohen, Y.E., 2013. The what , where and how of auditory-object perception. Nat. Publ. Gr. 14, 693–707. doi:10.1038/nrn3565

Botvinick, M.M., Braver, T.S., Barch, D.M., Carter, C.S., Cohen, J.D., 2001. Conflict Monitoring and Cognitive Control. Psychol. Rev. 108, 624–652. doi:10.1037//0033-295X.I08.3.624

Boucher, L., Palmeri, T.J., Logan, G.D., Schall, J.D., 2007. Inhibitory control in mind and brain: an interactive race model of countermanding saccades. Psychol. Rev. 114, 376–97. doi:10.1037/0033-295X.114.2.376

Brovelli, A., Ding, M., Ledberg, A., Chen, Y., Nakamura, R., Bressler, S.L., 2004. Beta oscillations in a large-scale sensorimotor cortical network: directional influences revealed by Granger causality. Proc. Natl. Acad. Sci. U. S. A. 101, 9849–54. doi:10.1073/pnas.0308538101

Canolty, R.T., Soltani, M., Dalal, S.S., Edwards, E., Dronkers, N.F., Nagarajan, S.S., Kirsch, H.E., Barbaro, N.M., Knight, R.T., 2007. Spatiotemporal dynamics of word processing in the human brain. Frontiers in Neuroscience, 1, 1, 185-196

Cardin, J. a, Carlén, M., Meletis, K., Knoblich, U., Zhang, F., Deisseroth, K., Tsai, L.-H., Moore, C.I., 2009. Driving fast-spiking cells induces gamma rhythm and controls sensory responses. Nature 459, 663–7. doi:10.1038/nature08002

Chamberlain, S.R., Fineberg, N. a, Blackwell, A.D., Robbins, T.W., Sahakian, B.J., 2006. Motor inhibition and cognitive flexibility in obsessive-compulsive disorder and trichotillomania. Am. J. Psychiatry 163, 1282–4. doi:10.1176/appi.ajp.163.7.1282

Chang, E.F., Rieger, J.W., Johnson, K., Berger, M.S., Barbaro, N.M., Knight, R.T., 2010. Categorical speech representation in human superior temporal gyrus. Nat. Neurosci. 13, 1428–32. doi:10.1038/nn.2641

Chikazoe, J., 2010. Localizing performance of go/no-go tasks to prefrontal cortical subregions. Curr. Opin. Psychiatry 23, 267–72. doi:10.1097/YCO.0b013e3283387a9f

Chikazoe, J., Jimura, K., Asari, T., Yamashita, K., Morimoto, H., Hirose, S., Miyashita, Y., Konishi, S., 2009. Functional dissociation in right inferior frontal cortex during performance of go/no-go task. Cereb. Cortex 19, 146–52.

doi:10.1093/cercor/bhn065

Clark, A., 2013. Whatever next? Predictive brains, situated agents, and the future of cognitive science. Behav. Brain Sci. 36, 181–204.

Comerchero, M.D., Polich, J., 1999. P3a and P3b from typical auditory and visual stimuli 110, 24–30.

Corbetta, M., Shulman, G.L., 2002. Control of goal-directed and stimulus-driven attention in the brain. Nat. Rev. Neurosci. 3, 201–15. doi:10.1038/nrn755

Coxon, J.P., Stinear, C.M., Byblow, W.D., 2006. Intracortical inhibition during volitional inhibition of prepared action. J. Neurophysiol. 95, 3371–83. doi:10.1152/jn.01334.2005

Crone, N.E., Miglioretti, D.L., Gordon, B., Lesser, R.P., 1998a. Functional mapping of human sensorimotor cortex with electrocorticographic spectral analysis. II. Event-related synchronization in the gamma band. Brain 121 (Pt 1, 2301–15.

Crone, N.E., Miglioretti, D.L., Gordon, B., Sieracki, J.M., Wilson, M.T., Uematsu, S., Lesser, R.P., 1998b. Functional mapping of human sensorimotor cortex with electrocorticographic spectral analysis. I. Alpha and beta event-related desynchronization. Brain 121 (Pt 1, 2271–99.

Czigler, I., Winkler, I., Pató, L., Várnagy, A., 2006. Visual temporal window of integration as revealed by the visual mismatch negativity event-related potential to stimulus omissions. Brain Res. 4, 129–140. doi:10.1016/j.brainres.2006.05.034

Delorme, A., Makeig, S., 2004. EEGLAB: an open source toolbox for analysis of single-trial EEG dynamics including independent component analysis. J. Neurosci. Methods 134, 9–21. doi:10.1016/j.jneumeth.2003.10.009

Dewitt, I., Rauschecker, J.P., 2013. Brain & Language Wernicke ' s area revisited : Parallel streams and word processing. Brain Lang. 127, 181–191. doi:10.1016/j.bandl.2013.09.014

Downar, J., Crawley, A.P., Mikulis, D.J., Davis, K.D., 2002. A cortical network sensitive to stimulus salience in a neutral behavioral context across multiple sensory modalities. J. Neurophysiol. 87, 615–620. doi:10.1152/jn.00636.2001

Downar, J., Crawley, a P., Mikulis, D.J., Davis, K.D., 2000. A multimodal cortical network for the detection of changes in the sensory environment. Nat. Neurosci. 3, 277–283. doi:10.1038/72991

Duann, J., Ide, J.S., Luo, X., Li, C.R., 2009. Functional Connectivity Delineates Distinct Roles of the Inferior Frontal Cortex and Presupplementary Motor Area in Stop Signal Inhibition. J. Neurosci. 29, 10171–10179. doi:10.1523/JNEUROSCI.1300-09.2009

Dürschmid, S., Edwards, E., Reichert, C., Dewar, C., Hinrichs, H., Heinze, H.-J., Kirsch, H.E., Dalal, S.S., Deouell, L.Y., Knight, R.T., 2016. Hierarchy of prediction errors for auditory events in human temporal and frontal cortex. Proc. Natl. Acad. Sci. 113, 6755–6760. doi:10.1073/pnas.1525030113

Edwards, E., Soltani, M., Deouell, L.Y., Berger, M.S., Knight, R.T., 2005. High gamma activity in response to deviant auditory stimuli recorded directly from human cortex. J. Neurophysiol. 94, 4269–80. doi:10.1152/jn.00324.2005

Engel, A.K., Fries, P., 2010. Beta-band oscillations--signalling the status quo? Curr. Opin. Neurobiol. 20, 156–65. doi:10.1016/j.conb.2010.02.015

Erika-Florence, M., Leech, R., Hampshire, A., 2014. A functional network perspective on response inhibition and attentional control. Nat. Commun. 5, 4073. doi:10.1038/ncomms5073

Flinker, a, Chang, E.F., Barbaro, N.M., Berger, M.S., Knight, R.T., 2011. Sub-centimeter language organization in the human temporal lobe. Brain Lang. 117, 103–9. doi:10.1016/j.bandl.2010.09.009

Folstein, J.R., Petten, C.V.A.N., 2008a. Influence of cognitive control and mismatch on the N2 component of the ERP : A review. Psychophysiology 45, 152–170. doi:10.1111/j.1469-8986.2007.00602.x

Folstein, J.R., Petten, C.V.A.N., 2008b. Influence of cognitive control and mismatch on the N2 component of the ERP : A review 45, 152–170. doi:10.1111/j.1469-8986.2007.00602.x

Foo, F., King-Stephens, D., Weber, P., Laxer, K., Parvizi, J., Knight, R.T., 2016. Differential Processing of Consonance and Dissonance within the Human Superior Temporal Gyrus. Front. Hum. Neurosci. 10, 154. doi:10.3389/fnhum.2016.00154

Ford, J.M., Hillyard, S.A., 1981. Event-related potentials (ERPs) to interruptions of a steady rhythm. Psychophysiology 18, 322–330.

Friston, K., 2010. The free-energy principle: a unified brain theory? Nat. Rev. Neurosci. 11, 127–138. doi:10.1038/nrn2787

Friston, K., 2009. The free-energy principle: a rough guide to the brain? Trends Cogn. Sci. 13, 293–301. doi:10.1016/j.tics.2009.04.005

Friston, K., 2005. A theory of cortical responses. Philos. Trans. R. Soc. Lond. B. Biol. Sci. 360, 815–36. doi:10.1098/rstb.2005.1622

Friston, K., Kiebel, S., 2009. Cortical circuits for perceptual inference. Neural Netw. 22, 1093–1104. doi:10.1016/j.neunet.2009.07.023

Fuster, J.M., 2013. Cognitive functions of the prefrontal cortex, in: Stuss, D.T., Knight, R.T. (Eds.), Principles of Frontal Lobe Function. Oxford University Press, pp. 11–22.

Garavan, H., Ross, T.J., Stein, E.A., 1999. Right hemispheric dominance of inhibitory control : An event-related functional MRI study. PNAS 96, 8301–8306.

Gazzaniga, M.S., Ivry, R.B., Mangun, G.R., 2002. Cognitive Neuroscience, the biology of the mind, Second. ed. W.W. Norton & Company.

Geng, J.J., Vossel, S., 2013. Re-evaluating the role of TPJ in attentional control: Contextual updating? Neurosci. Biobehav. Rev. 37, 2608–2620. doi:10.1016/j.neubiorev.2013.08.010

Gramfort, A., Luessi, M., Larson, E., Engemann, D.A., Strohmeier, D., Brodbeck, C., Goj, R., Jas, M., Brooks, T., Parkkonen, L., Hamalanen, M., 2013. MEG and EEG data analysis with MNE-Python. Front. Neurosci. 7, 1–13. doi:10.3389/fnins.2013.00267

Hamilton, L.S., Edwards, E., Chang, E.F., n.d. Parallel streams define the temporal dynamics of speech processing across human auditory cortex. doi:http://dx.doi.org/10.1101/097485

Hein, G., Knight, R.T., 2008. Superior temporal sulcus--It's my area: or is it? J. Cogn. Neurosci. 20, 2125–2136. doi:10.1162/jocn.2008.20148

Hermes, D., Miller, K.J., Wandell, B.A., Winawer, J., 2015. Gamma oscillations in visual cortex : The stimulus matters. Trends Cogn. Sci. 19, 57–58. doi:10.1016/j.tics.2014.12.009.Gamma

Hermes, D., Nguyen, M., Winawer, J., 2017. Neuronal synchrony and the relation between the blood-oxygen-level dependent response and the local field potential. PLOS Biol. 1–42.

Hickok, G., Poeppel, D., 2007. The cortical organization of speech processing. Nat. Rev. Neurosci. 8, 393–402. doi:10.1038/nrn2113

Hirose, S., Chikazoe, J., Jimura, K., Yamashita, K., Miyashita, Y., Konishi, S., 2009. NeuroImage Sub-centimeter scale functional organization in human inferior frontal gyrus. Neuroimage 47, 442–450. doi:10.1016/j.neuroimage.2009.04.094

Holdgraf, C.R., de Heer, W., Pasley, B., Rieger, J., Crone, N., Lin, J.J., Knight, R.T., Theunissen, F.E., 2016. Rapid tuning shifts in human auditory cortex enhance speech intelligibility. Nat. Commun. 7, 13654. doi:10.1038/ncomms13654

Hughes, H.C., Darcey, T.M., Barkan, H.I., Williamson, P.D., Roberts, D.W., Aslin, C.H., 2001. Responses of Human Auditory Association Cortex to the Omission of an Expected Acoustic Event. Neuroimage 1089, 1073–1089. doi:10.1006/nimg.2001.0766

Humphries, C., Liebenthal, E., Binder, J.R., 2010. NeuroImage Tonotopic organization of human auditory cortex. Neuroimage 50, 1202–1211. doi:10.1016/j.neuroimage.2010.01.046

Hwang, K., Ghuman, a. S., Manoach, D.S., Jones, S.R., Luna, B., 2014. Cortical Neurodynamics of Inhibitory Control. J. Neurosci. 34, 9551–9561. doi:10.1523/JNEUROSCI.4889-13.2014

Isoda, M., Hikosaka, O., 2008. Role for subthalamic nucleus neurons in switching from automatic to controlled eye movement. J. Neurosci. 28, 7209–18. doi:10.1523/JNEUROSCI.0487-08.2008

Janata, P., 2001. Brain Electrical Activity Evoked by Mental Formation of Auditory Expectations and Images 13, 169–194.

Jaramillo, S., Zador, A.M., 2011. Auditory cortex mediates the perceptual effects of acoustic temporal expectation. Nat. Neurosci. 14, 246–251. doi:10.1038/nn.2688.Auditory

Jasper, H., Penfield, W., 1949. Electrocorticograms in man : Effect of voluntary movement upon the electrical activity of the precentral gyrus. Zur Deutung des Norm. Elektrencephalogramms und seiner Veranderungen 183, 163–174.

Javitt, D.C., Steinschneider, M., Schroeder, E., Vaughan, H.G., Arezzo, J.C., 1994. Detection of stimulus deviance within primate primary auditory cortex : intracortical mechanisms of mismatch negativity (MMN) generation. Brain Res. 667, 192–200.

Johnson, R., 1993. On the neural generators of the P300 component of the event-related potential. Psychophysiology 30, 90–97.

Kalaska, J.F., Crammond, D.J., 1995. Deciding not to GO: neuronal correlates of response selection in a GO/NOGO task in primate premotor and parietal cortex. Cereb. Cortex 5, 410–28.

Kam, J.W.Y., Szczepanski, S.M., Canolty, R.T., Flinker, A., Auguste, K.I., Crone, N.E., Kirsch, H.E., Kuperman, R.A., Lin, J.J., Parvizi, J., Knight, R.T., 2016. Differential sources for 2 neural signatures of target detection: an electrocorticography study. Cereb. Cortex 1–12. doi:10.1093/cercor/bhw393

Kerns, J.G., Cohen, J.D., MacDonald, A.W., Cho, R.Y., Stenger, V.A., Carter, C.S., 2004. Anterior cingulate conflict monitoring and adjustments in control. Science 303, 1023–6. doi:10.1126/science.1089910

Knight, R.T., Scabini, D., 1998. Anatomic bases of event-related potentials and their relationship to novelty detection in humans. J. Clin. Neurophysiol. 15, 3–13.

Kok, P., Failing, M.F., de Lange, F.P., 2014. Prior expectations evoke stimulus templates in the primary visual cortex. J. Cogn. Neurosci. 26, 1546–1554.

Kok, P., Jehee, J.F.M., de Lange, F.P., 2012. Less Is More: Expectation Sharpens Representations in the Primary Visual Cortex. Neuron 75, 265–270.

Krämer, U.M., Knight, R.T., Münte, T.F., 2011. Electrophysiological evidence for different inhibitory mechanisms when stopping or changing a planned response. J. Cogn. Neurosci. 23, 2481–2493. doi:10.1162/jocn.2010.21573

Krämer, U.M., Solbakk, A.-K., Funderud, I., Løvstad, M., Endestad, T., Knight, R.T., 2013. The role of the lateral prefrontal cortex in inhibitory motor control. Cortex. 49, 837–49. doi:10.1016/j.cortex.2012.05.003

Lee, T.S., Mumford, D., 2003. Hierarchical Bayesian inference in the visual cortex. J. Opt. Soc. Am. 20, 1434. doi:10.1364/JOSAA.20.001434

Leonard, M.K., Baud, M.O., Sjerps, M.J., Chang, E.F., 2016. Perceptual restoration of masked speech in human cortex. Nat. Commun. 7, 13619. doi:10.1038/ncomms13619

Levitt, H., 1971. Transformed Up-Down Methods in Psychoacoustics. J. Acoust. Soc. Am. 49, 467–477.

Liegeois-Chauvel, C., Musolino, A., Badier, J.M., Marquis, P., Chauvel, P., 1994. Evoked potentials recorded from the auditory cortex in man : evaluation and topography of the middle latency components. Electroencephalogr. Clin. Neurophysiol. 92, 204–214.

Lijffijt, M., Kenemans, J.L., Verbaten, M.N., van Engeland, H., 2005. A meta-analytic review of stopping performance in attention-deficit/hyperactivity disorder: deficient inhibitory motor control? J. Abnorm. Psychol. 114, 216–22. doi:10.1037/0021-843X.114.2.216

Logan, G.D., Cowan, W.B., Davis, K. a, 1984. On the ability to inhibit simple and choice reaction time responses: a model and a method. J. Exp. Psychol. Hum. Percept. Perform. 10, 276–91.

Logothetis, N.K., Pauls, J., Augath, M., Trinath, T., Oeltermann, A., 2001. Neurophysiological investigation of the basis of the fMRI signal.

Mangun, G.R., 1995. Neural mechanisms of visual selective attention. Psychophysiology 32, 4–18.

Manning, J.R., Jacobs, J., Fried, I., Kahana, M.J., 2009. Broadband shifts in local field potential power spectra are correlated with single-neuron spiking in humans. J. Neurosci. 29, 13613–20. doi:10.1523/JNEUROSCI.2041-09.2009

Marco-Pallares, J., Camara, E., Mu, T.F., Rodrı, A., 2008. Neural Mechanisms Underlying Adaptive Actions after Slips. J. Cogn. Neurosci. 20, 1595–1610.

Maris, E., Oostenveld, R., 2007. Nonparametric statistical testing of EEG- and MEG-data □ , □□ 164, 177–190. doi:10.1016/j.jneumeth.2007.03.024

Markowitsch, H.J., Kalbe, E., Kessler, J., Markowitsch, H.J., Kalbe, E., Kessler, J., Stockhausen, H. Von, 1999. Short-Term Memory Deficit after Focal Parietal Damage Short-Term Memory Deficit after Focal Parietal Damage. J. Clin. Exp. Neuropsychol. 3395, 784–797. doi:10.1076/jcen.21.6.784.853

Martin, S., Brunner, P., Holdgraf, C., Heinze, H., Crone, N.E., Rieger, J., Schalk, G., Knight, R.T., Pasley, B.N., 2014. Decoding spectrotemporal features of overt and covert speech from the human cortex 7, 1–15. doi:10.3389/fneng.2014.00014

Matsuzaka, Y., Tanji, J., 1996. Changing Directions of Forthcoming Arm Movements : Neuronal. J. Neurophysiol. 76.

Mattia, M., Pani, P., Mirabella, G., Costa, S., Del Giudice, P., Ferraina, S., 2013. Heterogeneous attractor cell assemblies for motor planning in premotor cortex. J. Neurosci. 33, 11155–68. doi:10.1523/JNEUROSCI.4664-12.2013

Mattia, M., Spadacenta, S., Pavone, L., Quarato, P., Esposito, V., Sparano, a., Sebastiano, F., Di Gennaro, G., Morace, R., Cantore, G., Mirabella, G., 2012. Stop-event-related potentials from intracranial electrodes reveal a key role of

premotor and motor cortices in stopping ongoing movements. Front. Neuroeng. 5, 1–13. doi:10.3389/fneng.2012.00012

Miller, K.J., Hermes, D., Honey, C.J., Hebb, A.O., Ramsey, N.F., Knight, R.T., Ojemann, J.G., Fetz, E.E., 2012. Human motor cortical activity is selectively phase-entrained on underlying rhythms. PLoS Comput. Biol. 8, e1002655. doi:10.1371/journal.pcbi.1002655

Miller, K.J., Leuthardt, E.C., Schalk, G., Rao, R.P.N., Anderson, N.R., Moran, D.W., Miller, J.W., Ojemann, J.G., 2007. Spectral changes in cortical surface potentials during motor movement. J. Neurosci. 27, 2424–32. doi:10.1523/JNEUROSCI.3886-06.2007

Miller, K.J., Sorensen, L.B., Ojemann, J.G., Nijs, M. Den, 2009. Power-Law Scaling in the Brain Surface Electric Potential. PLoS Comput. Biol. 5, 1–10. doi:10.1371/journal.pcbi.1000609

Mirabella, G., 2014. Should I stay or should I go? Conceptual underpinnings of goal-directed actions. Front. Syst. Neurosci. 8, 1–21. doi:10.3389/fnsys.2014.00206

Mirabella, G., Iaconelli, S., Romanelli, P., Modugno, N., Lena, F., Manfredi, M., Cantore, G., 2012. Deep brain stimulation of subthalamic nuclei affects arm response inhibition in Parkinson's patients. Cereb. Cortex 22, 1124–32. doi:10.1093/cercor/bhr187

Mirabella, G., Pani, P., Ferraina, S., 2011. Neural correlates of cognitive control of reaching movements in the dorsal premotor cortex of rhesus monkeys. J. Neurophysiol. 106, 1454–66. doi:10.1152/jn.00995.2010

Mitra, P.P., Bokil, H., 2007. Observed brain dynamics. Oxford University Press.

Munakata, Y., Herd, S. a, Chatham, C.H., Depue, B.E., Banich, M.T., O'Reilly, R.C., 2011. A unified framework for inhibitory control. Trends Cogn. Sci. 15, 453–9. doi:10.1016/j.tics.2011.07.011

Murray, S.O., Kersten, D., Olshausen, B. a, Schrater, P., Woods, D.L., 2002. Shape perception reduces activity in human primary visual cortex. Proc. Natl. Acad. Sci. U. S. A. 99, 15164–9. doi:10.1073/pnas.192579399

Naatanen, R., Jiang, D., Lavikainen, J., Reinikainen, K., Paavilainen, P., 1993. Event-related potentials reveal a memory trace for temporal features. Neuroreport 5, 310–312.

Naatanen, R., Paavilainen, P., Rinne, T., Alho, K., 2007. The mismatch negativity

(MMN) in basic research of central auditory processing: A review. Clin. Neurophysiol. 118, 2544–2590. doi:10.1016/j.clinph.2007.04.026

Naatanen, R., Picton, T.W., 1986. N2 and automatic versus controlled processes. Cereb. Psychophysiol. Stud. event-related potentials 38, 169–105.

Neubert, F.-X., Mars, R.B., Rushworth, M.F.S., 2013. Is there an inferior frontal cortical network for cognitive control and inhibition?, in: Stuss, D.T., Knight, R.T. (Eds.), Principles of Frontal Lobe Function. Oxford university press, pp. 332–352.

Niessing, J., Ebisch, B., Schmidt, K.E., Niessing, M., Singer, W., Galuske, R. a W., 2005. Hemodynamic signals correlate tightly with synchronized gamma oscillations. Science 309, 948–51. doi:10.1126/science.1110948

Nordby, H., Hammerborg, D., Roth, W.T., Hugdahl, K., 1994. ERPs for infrequent omissions and inclusions of stimulus elements. Psychophysiology 31, 544–552.

Nunez, P.L., Srinivasan, R., 2006. Electric fields of the brain, the neurophysics of EEG, Second. ed. Oxford University Press.

Olshausen, B.A., 2014. Perception as an Inference Problem, in: Gazzaniga, M., Mangun, R. (Eds.), The Cognitive Neurosciences. MIT press, pp. 295–304.

Oostenveld, R., Fries, P., Maris, E., Schoffelen, J., 2011. FieldTrip : Open Source Software for Advanced Analysis of MEG , EEG , and Invasive Electrophysiological Data. Comput. Intell. Neurosci. 2011. doi:10.1155/2011/156869

Ozker, M., Schepers, I.M., Magnotti, J.F., Yoshor, D., Beauchamp, M.S., 2017. A double dissociation between anterior and posterior superior temporal gyrus for processing audiovisual speech demonstrated by electrocorticography. J. Cogn. Neurosci. doi:10.1162/jocn

Pasley, B.N., David, S. V, Mesgarani, N., Flinker, A., Shamma, S. a, Crone, N.E., Knight, R.T., Chang, E.F., 2012. Reconstructing speech from human auditory cortex. PLoS Biol. 10, e1001251. doi:10.1371/journal.pbio.1001251

Pfurtscheller, G., Lopes da Silva, F.H., 1999. Event-related EEG/MEG synchronization and desynchronization: basic principles. Clin. Neurophysiol. 110, 1842–57.

Pfurtscheller, G., Neuper, C., 1994. Event-related synchronization of mu rhythm in the EEG over the cortical hand area in man. Neurosci. Lett. 174, 93–96.

Picton, T.W., Hillyard, S.A., Galambos, R., 1974a. Cortical responses to omitted

stimuli, in: “Major Problems in Brain Electrophysiology” U.S.S.R.: Academy of Sciences.

Picton, T.W., Hillyard, S.A., Krausz, H.I., Galambos, R., 1974b. Human auditory evoked potentials. I: Evaluation of components. Electroencephalogr. Clin. Neurophysiol. 36, 179–190.

Polich, J., 2007. Updating P300 : An integrative theory of P3a and P3b. Clin. Neurophysiol. 118, 2128–2148. doi:10.1016/j.clinph.2007.04.019

Raij, T., Mcevoy, L., Makela, J.P., Hari, R., 1997. Human auditory cortex is activated by omissions of auditory stimuli. Brain Res. 745, 134–143.

Rao, R.P.N., Ballard, D.H., 1999. Predictive coding in the visual cortex : a functional interpretation of some extra-classical receptive-field effects 79–87.

Ray, N.J., Jenkinson, N., Brittain, J., Holland, P., Joint, C., Nandi, D., Bain, P.G., Yousif, N., Green, a., Stein, J.S., Aziz, T.Z., 2009. The role of the subthalamic nucleus in response inhibition: Evidence from deep brain stimulation for Parkinson’s disease. Neuropsychologia 47, 2828–2834. doi:10.1016/j.neuropsychologia.2009.06.011

Ray, S., Maunsell, J.H.R., 2011. Different origins of gamma rhythm and high-gamma activity in macaque visual cortex. PLoS Biol. 9, e1000610. doi:10.1371/journal.pbio.1000610

Rich, E.L., Wallis, J.D., 2017. Spatiotemporal dynamics of information encoding revealed in orbitofrontal high-gamma. Nature Communications 8, 1139. doi: 10.1038/s41467-017-01253-5

Rosburg, T., Trautner, P., Dietl, T., Korzyukov, O.A., Boutros, N.N., Schaller, C., Elger, C.E., Kurthen, M., 2005. Subdural recordings of the mismatch negativity (MMN) in patients with focal epilepsy. Brain 128, 819–828. doi:10.1093/brain/awh442

Sanmiguel, I., Saupe, K., Schröger, E., 2013. I know what is missing here: electrophysiological prediction error signals elicited by omissions of predicted “what” but not “when”. Front. Hum. Neurosci. 7, 407. doi:10.3389/fnhum.2013.00407

SanMiguel, I., Saupe, K., Schröger, E., 2013a. I know what is missing here: electrophysiological prediction error signals elicited by omissions of predicted ”what” but not ”when”. Front. Hum. Neurosci. 7, 407. doi:10.3389/fnhum.2013.00407

SanMiguel, I., Widmann, A., Bendixen, A., Trujillo-Barreto, N., Schröger, E., 2013b.

Hearing silences: human auditory processing relies on preactivation of sound-specific brain activity patterns. J. Neurosci. 33, 8633–9. doi:10.1523/JNEUROSCI.5821-12.2013

Scangos, K.W., Stuphorn, V., 2010. Medial Frontal Cortex Motivates But Does Not Control Movement Initiation in the Countermanding Task. J. Neurosci. 30, 1968–1982. doi:10.1523/JNEUROSCI.4509-09.2010

Schalk, G., McFarland, D.J., Hinterberger, T., Birbaumer, N., Wolpaw, J.R., 2004. BCI2000 : A General-Purpose Brain-Computer Interface (BCI) System. IEEE Trans. Biomed. Eng. 51, 1034–1043. doi:10.1109/TBME.2004.827072

Schall, J.D., Godlove, D.C., 2012. Current advances and pressing problems in studies of stopping. Curr. Opin. Neurobiol. 22, 1012–21. doi:10.1016/j.conb.2012.06.002

Schmidt, R., Leventhal, D.K., Mallet, N., Chen, F., Berke, J.D., 2013. Canceling actions involves a race between basal ganglia pathways. Nat. Neurosci. 16, 1118–24. doi:10.1038/nn.3456

Schnupp, J., Nelken, I., King, A., 2011. Auditory Neuroscience: making sense of sound. MIT press.

Serre, T., Oliva, A., Poggio, T., 2007. A feedforward architecture accounts for rapid categorization. Proc. Natl. Acad. Sci. U. S. A. 104, 6424–9. doi:10.1073/pnas.0700622104

Sharp, D.J., Bonnelle, V., Boissezon, X. De, Beckmann, C.F., James, S.G., Patel, M.C., Mehta, M.A., 2010. Distinct frontal systems for response inhibition , attentional capture , and error processing. PNAS 107, 6106–6111. doi:10.1073/pnas.1000175107

Shima, K., Mushiake, H., Saito, N., Tanji, J., 1996. Role for cells in the presupplementary motor area in updating motor plans. Proc. Natl. Acad. Sci. U. S. A. 93, 8694–8.

Simson, R., 1976. The scalp t o p o g r a p h y of potentials associated with missing visual o r auditory stimuli*. Electroencephalogr. Clin. Neurophysiol. 40, 33–42.

Snyder, E., Hillyard, S.A., 1976. Long-Latency Evoked Potentials to Irrelevant , Deviant Stimuli. Behav. Biol. 331, 319–331.

St. John-saaltink, E., Utzerath, C., Kok, P., Lau, H.C., 2015. Expectation Suppression in Early Visual Cortex Depends on Task Set. PLoS One 10, 1–14.

doi:10.7910/DVN/ZAELMD

Summerfield, C., Wyart, V., Johnen, V.M., Gardelle, V. De, 2011. Human scalp electroencephalography reveals that repetition suppression varies with expectation. Front. Hum. Neurosci. 5, 1–13. doi:10.3389/fnhum.2011.00067

Swann, N., Poizner, H., Houser, M., Gould, S., Greenhouse, I., Cai, W., Strunk, J., George, J., Aron, A.R., 2011. Deep brain stimulation of the subthalamic nucleus alters the cortical profile of response inhibition in the beta frequency band: a scalp EEG study in Parkinson's disease. J. Neurosci. 31, 5721–9. doi:10.1523/JNEUROSCI.6135-10.2011

Swann, N., Tandon, N., Canolty, R., Ellmore, T.M., McEvoy, L.K., Dreyer, S., DiSano, M., Aron, A.R., 2009. Intracranial EEG reveals a time- and frequency-specific role for the right inferior frontal gyrus and primary motor cortex in stopping initiated responses. J. Neurosci. 29, 12675–85. doi:10.1523/JNEUROSCI.3359-09.2009

Swann, N.C., Cai, W., Conner, C.R., Pieters, T. a, Claffey, M.P., George, J.S., Aron, A.R., Tandon, N., 2012a. Roles for the pre-supplementary motor area and the right inferior frontal gyrus in stopping action: electrophysiological responses and functional and structural connectivity. Neuroimage 59, 2860–70. doi:10.1016/j.neuroimage.2011.09.049

Swann, N.C., Tandon, N., Pieters, T. a, Aron, A.R., 2012b. Intracranial electroencephalography reveals different temporal profiles for dorsal- and ventro-lateral prefrontal cortex in preparing to stop action. Cereb. Cortex 23, 2479–88. doi:10.1093/cercor/bhs245

Swick, D., Ashley, V., Turken, U., 2011. Are the neural correlates of stopping and not going identical? Quantitative meta-analysis of two response inhibition tasks. Neuroimage 56, 1655–65. doi:10.1016/j.neuroimage.2011.02.070

Todorovic, A., van Ede, F., Maris, E., de Lange, F.P., 2011. Prior expectation mediates neural adaptation to repeated sounds in the auditory cortex: an MEG study. J. Neurosci. 31, 9118–23. doi:10.1523/JNEUROSCI.1425-11.2011

Tzvi, E., Fonken, Y.M., Crone, N.E., Chang, E.F., Parvizi, J., Knight, R.T., Krämer, U.M., 2013. Cross-frequency coupling in prefrontal and motor networks during inhibitory motor control, in: Annual Meeting of the Human Brain Mapping Organization.

van den Wildenberg, W.P.M., Burle, B., Vidal, F., van der Molen, M.W., Ridderinkhof,

K.R., Hasbroucq, T., 2010. Mechanisms and dynamics of cortical motor inhibition in the stop-signal paradigm: a TMS study. J. Cogn. Neurosci. 22, 225–39. doi:10.1162/jocn.2009.21248

van den Wildenberg, W.P.M., van Boxtel, G.J.M., van der Molen, M.W., Bosch, D.A., Speelman, J.D., Brunia, C.H.M., 2006. Stimulation of the Subthalamic Region Facilitates the Selection and Inhibition of Motor Responses in Parkinson's Disease. J. Cogn. Neurosci. 18, 626–636. doi:10.1162/jocn.2006.18.4.626

Verbruggen, F., Logan, G.D., Liefooghe, B., Vandierendonck, A., 2008. Short-term aftereffects of response inhibition: repetition priming or between-trial control adjustments? J. Exp. Psychol. Hum. Percept. Perform. 34, 413–26. doi:10.1037/0096-1523.34.2.413

Wacongne, C., Changeux, J., Dehaene, S., 2012. A Neuronal Model of Predictive Coding Accounting for the Mismatch Negativity. J. Neurosci. 32, 3665–3678. doi:10.1523/JNEUROSCI.5003-11.2012

Wacongne, C., Labyt, E., Wassenhove, V. van, Bekinschtein, T., Naccache, L., Dehaene, S., 2011. Evidence for a hierarchy of predictions and prediction errors in human cortex. Proc. Natl. Acad. Sci. 108, 20754–20759. doi:10.1073/pnas.1117807108

Yabe, H., Tervaniemi, M., Sinkkonen, J., Huotilainen, M., Ilmoniemi, R.J., Näätänen, R., 1998. Temporal window of integration of auditory information in the human brain. Psychophysiology 35, 615–619. doi:10.1017/S0048577298000183

Zandbelt, B.B., Vink, M., 2010. On the role of the striatum in response inhibition. PLoS One 5. doi:10.1371/journal.pone.0013848

Zhang, Y., Chen, Y., Bressler, S.L., Ding, M., 2008. Response preparation and inhibition: the role of the cortical sensorimotor beta rhythm. Neuroscience 156, 238–46. doi:10.1016/j.neuroscience.2008.06.061

Zola-Morgan, S., 1995. Localization of brain function: the legacy of Franz Joseph Gall (1758-1828). Annu. Rev. Neurosci. 18, 359–383.

Appendices

Appendix A: Tables

Table 2.1: Demographic and clinical data Chapter 2

Subject	Age (years)	Sex	Handedness	Epileptic focus
S01	23	M	R	None found/unknown
S02	22	M	R	Left parietal lesion, fronto-polar contusion
S03	42	M	L	Left superior temporal cortex
S04	30	M	R	Left Orbitofrontal cortex
S05	14	M	R	None found/unknown
S06	27	F	R	Left anterior temporal cortex
S07	20	M	L	None found/unknown
S08	42	M	L	Posterior cingulate cortex

Table 2.3: Behavioral data Chapter 2

Subject	Go-RT	US-RT	SSD-SS	SSD-US	SSRT	Probability of Failure (%)	PostUS-RT change	PostSS-RT change
S01	635	495	351	355	219	41	66	-133
S02	517	454	183	202	316	49	49	-36
S03	502	427	212	235	256	52	97	-109
S04	501	374	192	213	268	53	90	-94
S05			140	160		49		
S06	430	406	108	128	294	50	51	24
S07	443	392	141	166	271	49	21	-21
S08	661	560	155	170	474	52	41	-76
Mean ±SEM	**526 ± 34**	**445 ± 25**	**185 ± 26**	**204 ± 25**	**302 ± 31**	**49.4 ± 1.3**	**59 ± 10**	**-64 ± 21**

Go reaction time (Go-RT), stop-error reaction time (US-RT), stop signal delay in unsuccessful (SSD-US) and successful stop-trials (SSD-SS), stop signal reaction time (SSRT) and the difference in Go response time after compared to before an unsuccessful stop trial (postUS-slowing) or a successfully inhibited stop-trial (postSS-slowing) in ms. Due to technical issues some of the behavioral data for S05 was lost.

Table 3.1: Subject demographic information, Chapters 3 and 4. * denotes unknown

Subject	Gender	Age	Handedness	Hand used	Language lateralization	Seizure focus
AB62	F	33	Right	Left	*	*
AB71	M	57	Left	Left	Left	*
AB78	M	69	Right	Left	*	anterior ventro-temporal
AB79	M	31	Right	Right	*	potentially ventral/temporal pole
AB81	M	33	Right	Right	Left (wada)	anterior depth (HC?)
IR39	M	34	Ambidextrous	Right	*	Bilateral hippocampus

Table 3.2: Behavioral data per subject, Chapters 3 and 4. Reaction times to targets in seconds, hits in percentage, misses and false alarms in number of trials total.

Subjects	**RT median (ms)**	**RT mean (ms)**	**RT standard deviation (ms)**	**Hits**	**Misses (# trials)**	**False alarms (# trials)**
AB62	643	661	224	98%	1	1
AB71	438	481	160	81%	9	43
AB78	550	578	147	92%	4	4
AB79	500	528	122	96%	2	1
AB81	527	563	193	85%	7	2
IR39	481	503	91	86%	0	4
Average	**523**	**552**	**156**	**90%**		